

Developing a novel bioink from hyaluronic acid-alginate-silk
fibroin (HA- Alg-SF) for cartilage 3D printing

Miss Truc Thanh Nguyen



A Thesis Submitted in Partial Fulfillment of the Requirements
for the Degree of Master of Science in Medical Sciences
Common Course
FACULTY OF MEDICINE
Chulalongkorn University
Academic Year 2020
Copyright of Chulalongkorn University

การพัฒนาหมึกพิมพ์ชีวภาพจากไฮyalูโรนิกแอซิด-แอลจีเนต-โปรตีนไฟโบรอิน (HA-ALG-SF) สำหรับการพิมพ์กระดูกอ่อนแบบสามมิติ



วิทยานิพนธ์นี้เป็นส่วนหนึ่งของการศึกษาตามหลักสูตรปริญญาวิทยาศาสตรมหาบัณฑิต
สาขาวิชาวิทยาศาสตร์การแพทย์ ไม่สังกัดภาควิชา/เทียบเท่า
คณะแพทยศาสตร์ จุฬาลงกรณ์มหาวิทยาลัย
ปีการศึกษา 2563
ลิขสิทธิ์ของจุฬาลงกรณ์มหาวิทยาลัย

Thesis Title	Developing a novel bioink from hyaluronic acid-alginate-silk fibroin (HA- Alg-SF) for cartilage 3D printing
By	Miss Truc Thanh Nguyen
Field of Study	Medical Sciences
Thesis Advisor	Dr. Supansa Yodmuang, Ph.D.
Thesis Co Advisor	Assistant Professor JITTIMA LUCKANAGUL, Pharm.D, Ph.D

Accepted by the FACULTY OF MEDICINE, Chulalongkorn University in
Partial Fulfillment of the Requirement for the Master of Science

----- Dean of the FACULTY OF
MEDICINE
(Professor SUTTIPONG WACHARASINDHU, M.D)

THESIS COMMITTEE

----- Chairman
(Associate Professor POONLARP CHEEPSUNTHORN,
Ph.D)

----- Thesis Advisor
(Dr. Supansa Yodmuang, Ph.D.)

----- Thesis Co-Advisor
(Assistant Professor JITTIMA LUCKANAGUL,
Pharm.D, Ph.D)

----- Examiner
(Assistant Professor DEPICHA JINDATIP, Ph.D.)

----- External Examiner
(Assistant Professor Phornphop Naiyanetr, Ph.D.)

จุฬาลงกรณ์มหาวิทยาลัย
CHULALONGKORN UNIVERSITY

ตริก ฐานท์ เหยียน : การพัฒนาหมึกพิมพ์ชีวภาพจากไฮยาลูโรนิกแอซิด-แอลจีเนท-โปรตีนไฟโบรอิน (HA-ALG-SF) สำหรับการพิมพ์กระดูกอ่อนแบบสามมิติ. (Developing a novel bioink from hyaluronic acid-alginate-silk fibroin (HA- Alg-SF) for cartilage 3D printing) อ.ที่ปรึกษาหลัก : สุพรรณษา ยอดเมือง, อ.ที่ปรึกษาร่วม : จิตติมา ลักคณากุล

ในการพัฒนาหมึกชีวภาพสำหรับการพิมพ์ 3 มิติของกระดูกอ่อนจากกรดไฮยาลูโรนิก (HA) และโซเดียมอัลจีเนต (Alg) ที่ถูกดัดแปลงเป็นกรดเอมีน-ไฮยาลูโรนิก (HA-NH₂) และอัลดีไฮด์อัลจีเนต (Alg-CHO) นั้น เทคนิคนิวเคลียร์แมกเนติก เรโซแนนซ์สเปกโตรสโคปี (NMR) และฟูเรียร์ทรานส์ฟอร์มอินฟราเรดสเปกโตรสโคปี (FT-IR) ได้ยืนยันการดัดแปลงโครงสร้างของ HA-NH₂ และ Alg-CHO ที่ประสบความสำเร็จ ไฮโดรเจลกรดไฮยาลูโรนิกที่ดัดแปลงและอัลดีไฮด์อัลจีเนต (HA-Alg) เกิดขึ้นจากปฏิกิริยาดีไฮเดรชันได้เป็นอิมินระหว่างเอมีนปฐมภูมิและอัลดีไฮด์เพื่อสร้างพันธะอิมิน ซึ่งอัตราส่วน 5:5 ของหมึกชีวภาพที่เป็นผลลัพท์ของไฮโดรเจล HA-Alg ที่เหมาะสมที่สุด แสดงถึงความสามารถในการพิมพ์ ความเข้ากันได้ทางชีวภาพ และการทำงานเป็นหมึกชีวภาพสำหรับเนื้อเยื่อกระดูกอ่อน ไฮโดรเจล HA-Alg ที่อัตราส่วน 5:5 พิมพ์โดยเครื่องพิมพ์ 3 มิติแบบอเล็กซ์ที่กำหนดเอง มีการเชื่อมสภาพซ้ำ มีการไหลที่ต่ำ ความหนืดเฉือนลดลงตามอัตราเฉือน สามารถสนับสนุนความอยู่รอดของเซลล์ การเพิ่มจำนวนเซลล์ และการพัฒนาของเซลล์กระดูกอ่อน เพื่อพิสูจน์ว่า HA-Alg สามารถทำหน้าที่เป็นแทนสำหรับการคักจับของโมเลกุลขนาดใหญ่ ซิลค์ไฟโบรอิน (SF) ถูกบรรจุเข้าไปในสูตรผสม HA-Alg เพื่อพัฒนาไฮโดรเจล HA-Alg-SF ผลการทดลองแสดงให้เห็นว่า ไฮโดรเจล HA-Alg-SF สามารถปรับให้เข้ากับการพิมพ์ 3 มิติได้ และส่งเสริมการสร้างเนื้อเยื่อกระดูกอ่อน การเติม SF ไม่ได้ทำให้ความสามารถในการพิมพ์และความอยู่รอดของเซลล์ในไฮโดรเจล HA-Alg-SF ลดลง เมื่อเปรียบเทียบกับไฮโดรเจล HA-Alg ซึ่งเสนอแนะว่าไฮโดรเจล HA-Alg อาจเป็นพอลิเมอร์เชื่อมโยงโครงร่างดาข่ายสำหรับการผสมกับโปรตีนอื่นๆ และสารส่งผลต่อปัจจัยการเจริญเติบโต สำหรับการใช้งานในด้านอื่นๆ ต่อไป



สาขาวิชา วิทยาศาสตร์การแพทย์
ปีการศึกษา 2563

ลายมือชื่อนิสิต

ลายมือชื่อ อ.ที่ปรึกษาหลัก

ลายมือชื่อ อ.ที่ปรึกษาร่วม

6278008830 : MAJOR MEDICAL SCIENCES

KEYWORD Hyaluronic acid, Alginate, 3D printing, bioink, cartilage tissue
D:

Truc Thanh Nguyen : Developing a novel bioink from hyaluronic acid-alginate-silk fibroin (HA- Alg-SF) for cartilage 3D printing. Advisor: Dr. Supansa Yodmuang, Ph.D. Co-advisor: Asst. Prof. JITTIMA LUCKANAGUL, Pharm.D, Ph.D

In the development of a bioink for cartilage 3D printing, Hyaluronic acid (HA), Alginate (Alg) were modified into amine-hyaluronic acid (HA-NH₂) and aldehyde alginate (Alg-CHO). Magnetic Nuclear Resonance (NMR) and Fourier Transform Infrared Spectroscopy (FTIR) confirmed the successful modification of HA-NH₂ and Alg-CHO. The hydrogel HA-Alg was crosslinked as a result of Schiff's base reaction, between primary amines and aldehydes to form imine bonds. By varying volume ratios, the optimal hydrogel HA-Alg (5:5) exhibited its printability, biocompatibility, and functionality as a bioink for cartilage tissue. HA-Alg (5:5) was printable with a custom-made extrusion 3D printer, had slow degradation, shear-thinning behavior, supported cell viability, proliferation, and chondrogenic differentiation. To prove that HA-Alg could act as a platform for entrapment of macromolecules, Silk fibroin (SF) which is a biocompatible protein was loaded into HA-Alg formulation to develop HA-Alg-SF hydrogel. The results showed that HA-Alg-SF hydrogel adapted to 3D printing, and promoted cartilage tissue formation. The addition of SF did not compromise the printability and cell viability of HA-Alg-SF hydrogel comparing to HA-Alg hydrogel, which suggested that HA-Alg hydrogel could be an interpenetrating polymer network (IPN) for loading other proteins, and growth factors for further applications.



Field of Study: Medical Sciences

Student's Signature

Academic 2020

.....
Advisor's Signature

Year:

.....
Co-advisor's Signature

.....

ACKNOWLEDGEMENTS

I would like to express my deepest gratitude to my advisor, Dr. Supansa Yodmuang who supported me a lot during my thesis. Without my advisor, I could not complete my thesis, her willingness and insightful guidance have helped me overcome the challenges during the journey. My special thanks goes to Dr. Depicha Jindatip and her lab members for their support in my histology experiments. I would like to thank Dr. Jittima Lukanagul who gave me the opportunity to use the facilities in Department of Pharmaceutical Sciences. I am extremely thankful to members of examination committees, Associate Professor. Poonlarp Cheepsunthorn, Dr. Supansa Yodmuang, Dr. Depicha Jindatip, Dr. Jittima Lukanagul, and Dr. Phornphop Naiyanetr for valuable suggestions in my thesis.

I would like to express my special thanks to my labmates, Ms. Pensuda Sompunga, Mr. Nattapak Damuras, and all SY Lab members for their help in all matters.

I own my deepest gratitude to my parents for their love and support throughout the years.

I would like to thank Ms. Apinya Butlee, Graduate Affairs, Faculty of Medicine for her student support.

Lastly, I extremely appreciate Graduate School of Chulalongkorn University and acknowledge ASEAN Scholarship for granting me to pursue my degree.

Truc Thanh Nguyen

TABLE OF CONTENTS

	Page
ABSTRACT (THAI)	iii
ABSTRACT (ENGLISH).....	iv
ACKNOWLEDGEMENTS	v
TABLE OF CONTENTS.....	vi
LIST OF TABLES	ix
LIST OF FIGURES	x
CHAPTER 1	1
INTRODUCTION	1
1.1 Background and rationale	1
1.2 Research questions.....	2
1.3 Hypothesis	2
1.4 Objectives	2
1.5 Expected benefits and applications.....	3
1.6 Conceptual framework.....	3
CHAPTER 2	4
LITERATURE REVIEW	4
2.1 3D printing technology in tissue engineering.....	4
2.2 Extrusion-based	5
2.3 Bioink	6
2.3.1 Silk fibroin-based bioink.....	7
2.3.2 Hyaluronic acid-based bioink.....	7
2.3.3 Alginate	8
CHAPTER 3	10
RESEARCH METHODOLOGY.....	10
3.1 Materials	10

3.2 Synthesis of amine hyaluronic acid (HA-NH ₂):	10
3.3 Synthesis of aldehyde-modified alginate (Alg-CHO):	11
3.4 Preparation of silk fibroin	11
3.5 Fabrication of the HA-Alg hydrogel.....	11
3.6 Fabrication of HA-Alg-SF hydrogel.....	11
3.7 Characterization of HA-Alg and HA-Alg-SF hydrogel.....	12
3.7.1 Nuclear Magnetic Resonance (NMR) analysis	12
3.7.2 Fourier transform infrared spectroscopy (FTIR) analysis	12
3.7.3 Swelling and degradation analysis	12
3.7.4 Rheological properties of hydrogels.....	12
3.7.5 Mechanical Assessment of hydrogels	13
3.7.6 Printability of HA-Alg (5:5) and HA-Alg-SF	13
3.7.7 Cytotoxicity and biocompatibility evaluation of hydrogels	13
3.7.7.1 Sample sterilization	14
3.7.7.2 <i>Cell culture and cell encapsulation in hydrogels</i>	14
3.7.7.3 <i>Live/dead assay</i>	14
3.7.7.4 <i>Quant-iT™ Picogreen™ dsDNA Assay</i>	14
3.7.7.5 <i>PrestoBlue™ assay</i>	15
3.7.7.6 <i>Ki-67 staining</i>	15
3.7.8 Cartilage tissue development.....	15
3.7.8.1 <i>Chondrogenic differentiation</i>	15
3.7.8.2 <i>Immunofluorescent staining</i>	16
3.8. Statistical analysis.....	16
CHAPTER 4	17
DATA ANALYSIS AND INTEPRETATION.....	17
4.1 NMR analysis of HA-NH ₂ and Alg-CHO	17
4.2 FTIR analysis of HA-NH ₂ , Alg-CHO and HA-Alg hydrogels.....	19
4.3 Gelation of HA-Alg at varied volume ratio and HA-Alg-SF.	19
4.4 Swelling and degradation behavior of hydrogels	21

4.5 3D Printing of HA-Ag (5:5) and HA-Alg-SF bioinks	23
4.6 Compressive strength of hydrogels	24
4.7 Rheological properties	25
4.8 In vitro cytocompatibility of HA-Alg and HA-Alg-SF hydrogels.....	27
4.8.1 In vitro live/dead.....	27
4.8.2 Quant-iT™ Picogreen™ dsDNA Assay.....	28
4.8.3 PrestoBlue™ assay	29
4.8.4 Immunochemical staining of Ki-67	30
4.9 Cell differentiation in HA-Alg (5:5) and HA-Alg-SF hydrogels	31
CHAPTER 5	33
CONCLUSION, DISCUSSION, AND RECOMMENDATIONS	33
5.1 Major findings	33
5.2 Discussion.....	33
5.3 Limitation of the study.....	37
REFERENCES	38
VITA.....	43

LIST OF TABLES

	Page
<i>Table 1 . Formulation of HA-Alg hydrogel at varied volume ratio.</i>	20
<i>Table 2. Weight difference (%) of hydrogels in PBS for 60 days.</i>	22



LIST OF FIGURES

	Page
<i>Figure 1. Extrusion-based 3D printing technique [25].</i>	6
<i>Figure 2. ¹H-NMR spectra of pure HA and modified HA-NH₂.</i>	17
<i>Figure 3. A) Oxidation of alginate by sodium periodate and the formation of intermolecular hemiacetal, B) ¹H-NMR spectra of pure Alg and modified Alg-CHO, C) ¹³C-NMR spectra of pure Alg and modified Alg-CHO.</i>	18
<i>Figure 4. FTIR analysis of A) HA, HA-NH₂, Alg, Alg-CHO, and B) extracted SF, HA-Alg (5:5), HA-Alg-SF hydrogels.</i>	19
<i>Figure 5. HA-Alg hydrogel at different volume ratios and HA-Alg-SF hydrogel made from HA-Alg (5:5).</i>	21
<i>Figure 6. Swelling and degradation profiles of HA-Alg and HA-Alg-SF hydrogels (mean±SD).</i>	23
<i>Figure 7. A) Custom-made 3D printer (Enterprise 2.0) B) 3D printing of HA-Alg (5:5), C) Printing of HA-Alg (5:5) and HA-Alg-SF hydrogels with hMSCs loading ..</i> 24	
<i>Figure 8. Compressive strength of hydrogels A) Recovery ability of HA-Alg (5:5) after compression, B) Typical compressive stress-strain curve of HA-Alg (5:5) and HA-Alg-SF hydrogels, C) The elastic modulus of HA-Alg and HA-Alg-SF hydrogels.</i>	25
<i>Figure 9. Rheological analysis of HA-Alg and HA-Alg-SF hydrogel a) Strain sweep, B) Frequency sweep, C) Time sweep, D) Shear-thinning properties of HA-Alg (5:5) and HA-Alg-SF.</i>	27
<i>Figure 10. Live/Dead staining of hMSCs encapsulated in 3D HA-Alg (5:5) and HA-Alg-SF hydrogels in 1, 3, 7 days, (scale bars=500 μm).</i>	28
<i>Figure 11. Quant-iT™ Picogreen™ dsDNA Assay. A) Standard curve, B) DNA amount detected from HA-Alg (5:5) and HA-Alg-SF hydrogels comparing with Fibrin.</i>	29
<i>Figure 12. PrestoBlue™ assay in cell proliferation of HA-Alg (5:5), HA-Alg-SF, and Fibrin hydrogels after 1, 3, 7 days.</i>	30
<i>Figure 13. Immunohistochemical staining of Ki67 in HA-Alg (5:5) and HA-Alg-SF hydrogels after 7 days of cell culture, (scale bars=200μm).</i>	31

Figure 14. Immunostaining of type II Collagen in HA-Alg (5:5) and HA-Alg-SF hydrogel after 2 weeks and 4 weeks. Negative control was stained without primary antibody (scale: 200 μm).32



CHAPTER 1

INTRODUCTION

1.1 Background and rationale

Organ and tissue transplantation helps save and improve millions of patients every year. However, it is reported that only 10% of need for organ transplantation is being met, followed the World Health Organization (Geneva). This organ shortage has become one of key factors that leads to development of tissue engineering and regenerative medicine. Tissue engineering is defined as "an interdisciplinary field which applies the principles of engineering and life sciences towards the development of biological substitutes that aim to maintain, restore or improve tissue function" [1]. The advances in tissue engineering in recent years have brought new hope to the patients with organ failure or tissue injuries without self-healing capacity. One of most advanced technology in tissue engineering and regenerative medicine now is 3D bioprinting, which can provide biomimetic complex tissues and organs thanks to integration of computer modelling. Herein, bioink is the key component that determines all characteristics of printed construct. The findings of printable, 3D structure forming, and biological compatible bioinks are being of interest in recent years [2, 3].

Cartilage which is one of most common tissues being studied since it cannot self-regenerate and mostly requires support from medical intervention. To promote the concept of lab-grown cartilage by 3D printing, this study aimed to develop cartilage bioink from natural polymers consisting of Hyaluronic acid (HA), alginate (Alg), and silk fibroin (SF). These three materials are popularly used in tissue engineering and regenerative medicine because they are biocompatible and can be modified to crosslink hydrogels. Taking the advantages of hydrogel's viscoelasticity and compatibility, the fabricated bioink was expected to favor printing process and tissue culture. To induce the gelation, HA and Alg were modified with new functional groups. HA was reacted with carbodiimide to activate its carboxyl groups, then these carboxyl groups could react with amino group of a diamine to form amino hyaluronic derivative [4]. On the other hand, Alg was oxidized with sodium periodate (NaIO_4) at the second and third carbon positions (C-2 and C-3) of its subunits, resulting in the

formation of two new aldehyde groups [5]. Amino-modified hyaluronic acid (HA-NH₂) and aldehyde alginate (Alg-CHO) were mixed to form HA-Alg hydrogel. The crosslink mechanism of HA-Alg hydrogel was due to reaction between amino and aldehyde groups, also called Schiff's base reaction [6].

Together with HA and Alg, SF gains much attentions as a protein polymer for cartilage regeneration. SF from silkworms has unique properties of low immunogenicity, impressive mechanical strength, biocompatibility, and especially slow degradation rate. Unfortunately, SF hydrogel is poor printability [7, 8]. Combination of SF solution with HA and Alg to form HA-Alg-SF bioink was considered as an effective approach to adjust rheological properties and investigated whether SF could improve the physical properties and biocompatibility of bioink. The composite HA-Alg and HA-Alg-SF were characterized by magnetic nuclear resonance (NMR), Fourier Transformed Infrared Spectroscopy (FTIR), rheological analysis, compressive strength and degradation test. Then, the biocompatibility was also examined with live/dead staining, cell viability, and cell proliferation assay. Finally, HA-Alg and HA-Alg-SF hydrogels in supporting chondrogenic differentiation were also figured out.

1.2 Research questions

Can Hyaluronic acid, Alginate, and Silk fibroin be a printable bioink for extrusion-based 3D printer and support cartilage formation?

1.3 Hypothesis

Does HA-Alg-SF hydrogel outweigh HA-Alg hydrogel in printing and support tissue formation?

1.4 Objectives

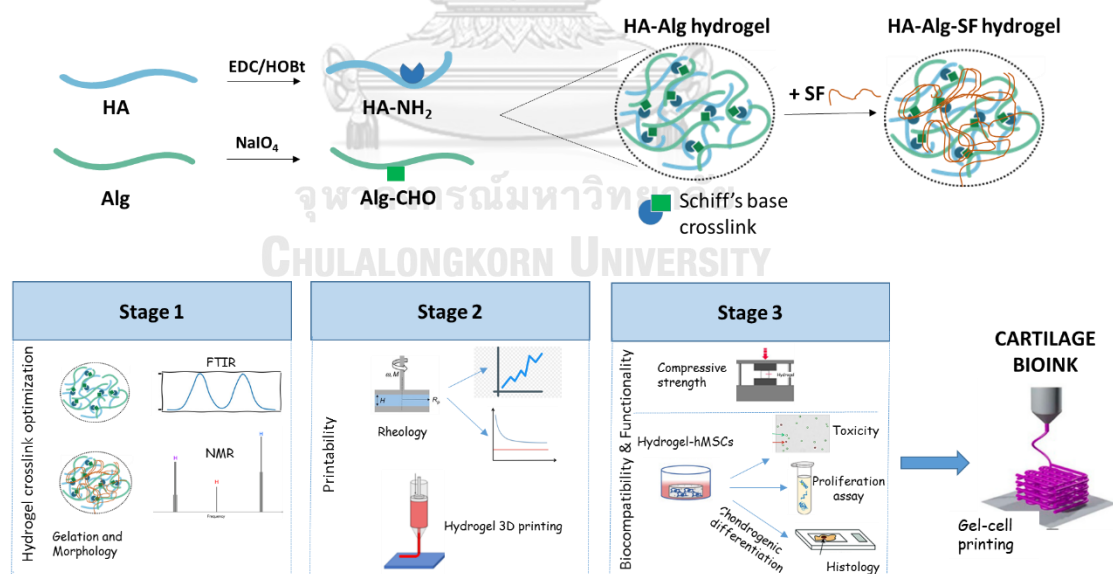
The goal of this research is to modify the chemical structure of Hyaluronic acid, Alginate to fabricate HA-Alg hydrogel, and added Silk fibroin into HA-Alg network, to create HA-Alg-SF bioink for a custom-made 3D extruded-printer. Specific objectives are:

- Developing the procedure for chemical modification HA and Alg in order to crosslink HA and Alg to become hydrogel.
- Optimizing the ratio between HA and Alg to result in a stiff and printable hydrogels.
- Adding SF into optimal HA-Alg formulation, then comparing the printability and biological characteristics between HA-Alg and HA-Alg-SF hydrogels.

1.5 Expected benefits and applications

3D bioprinting is a big progress of tissue engineering and regenerative medicine, which allows the production of complex tissue constructs for organ repair and replacement. The current limitation of 3D bioprinting is lack of a printable and biocompatible bioink, which adapts to both printing technique and in vitro condition. A project of bioink development is one of the utmost concerns of the scientists, among which is the formulation of HA-Alg-SF hydrogel bioink for cartilage regeneration.

1.6 Conceptual framework



CHAPTER 2

LITERATURE REVIEW

2.1 3D printing technology in tissue engineering

Tissues are constituted by cells, extracellular matrix (ECM) and signaling molecules. ECM provides the anchorage for cells and serves as a dynamic system that transmit the specific signals from growth factors, hormones, cytokines to the target cells that affects cell behavior. Since ECM is a 3D network of collagen, elastic fibers containing proteoglycans, adhesive proteins and glycoaminoglycans, tissue engineering allows the fabrication of artificial ECM or biomimetic scaffolds which provide structural support for new tissue formation inside or outside the body [9, 10]. Tissue engineering, the interdisciplinary field of material sciences, biochemistry, and physics, as reviewed today, has focused on the idea of creating 3D scaffolds incorporating with multiple cell types to repair or replace damaged tissues and organs [11]. For decades, conventional methods in fabricating scaffolds such as lyophilization, electrospinning, salt leaching and in situ crosslinked hydrogels have achieved limited success in investigating the biocompatibility of natural and synthetic materials for cell growth and tissue formation, but remain deficient in creating intricate 3D tissue structures. Additionally, the cells seeded onto scaffolds' surface after fabrication may not migrate in towards the center and may not be homogeneously distributed inside the scaffolds [12, 13].

To overcome the drawbacks of conventional manufacturing techniques, three-dimensional (3D) printing has been proposed to fabricate customized scaffolds that are highly desirable for clinical applications. 3D printing in tissue engineering involves using a 3D printer to print a construct generated by computer-aided-design or manufacturing (CAD/CAM), through layer-by-layer deposition of bioink. The printing paths, infill density, and layer's height can be determined prior to printing process and enable the production of precisely microporous scaffolds with well-defined 3D geometry. Multiple cell types are also distributed throughout the printed constructs in a controlled manner. It is considered that fabrication of biomimetic scaffolds using 3D printing technique is more flexible designed and patient-specific [14, 15].

The four primary 3D printing techniques utilized in tissue engineering are extrusion-based, injek-based, laser-assisted and stereolithography [16].

2.2 Extrusion-based

Extrusion-based bioprinting is considered as the most common in tissue engineering. This technique involves the dispersion of materials in the form of powder, hydrogels or cell aggregation using the extrusion nozzle incorporated with 3D motion. Most extrusion bioprinters comprise multiple print heads that are flexible for printing multiple materials within one single construct. Depending on the thermoplasticity of printed materials, also known as bioinks, extrusion-based bioprinting is categorized into two types: Fused deposition modeling (FDM) and pressure-assisted microsyringe (PAM) [17, 18].

FDM relates to the printing of thermoplastic materials in form of granules, fibers, or powder that require melting and liquefying into flow materials before extrusion. The melting process is usually manipulated by heating the print head or cartridge containing these polymer. Subsequently, the melted polymers are extruded through the syringe nozzle by a screw-driven or pneumatic air pressure system. FDM is advantage for manufacturing and ensuring the maintenance of the mesh and rigid scaffolds. However, the high temperature required during the process can decrease cell viability. Cell-free polycaprolactone (PCL) or poly-lactic acid (PLA) printing are typical examples of using FDM, and have been used to generate supporting structure for hydrogel printing [18-20].

Another type of extrusion-based bioprinting is PAM. The starting material for this technique is usually a viscous bioink, which can be expelled from the nozzle by pressurized air or rotating screw at room temperature or lower [21]. Crosslinked hydrogels can meet requirements of bioinks for PAM, which have semisolid formulation and the property to form a 3D structure without collapsing during and after printing process [22]. In this technique, the most important parameter is printability depending mainly on the bioink viscosity. If the viscosity is too high, bioink will be clogged in the nozzle. If the viscosity is too low, the printed layer will be deformed and collapsed [23]. In case of hydrogels encapsulated with cell, the generated high pressure and shear force may also affect the cell viability [24]. The

investigation of hydrogel bioinks possessing biocompatibility and appropriate viscosity is now of interest to many tissue engineers.

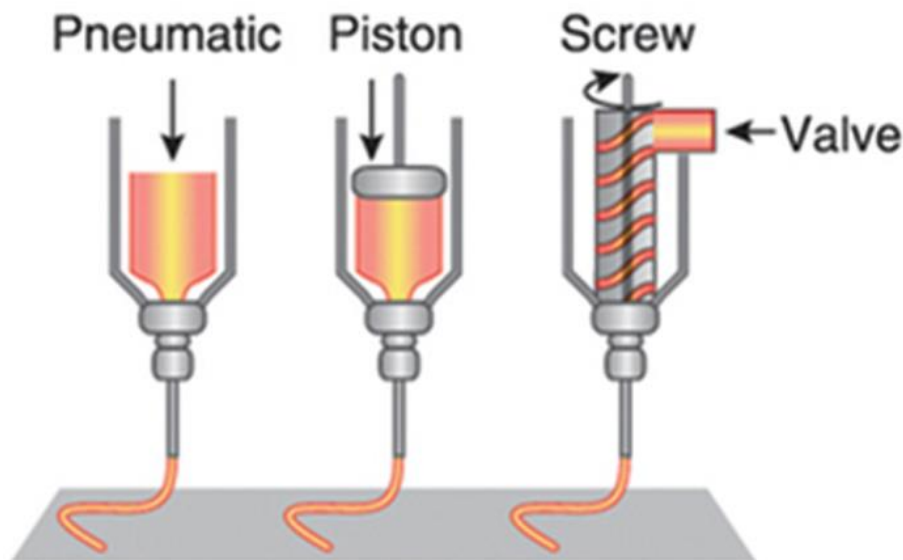


Figure 1. Extrusion-based 3D printing technique [25].

2.3 Bioink

Bioink is the material used for printing the 3D scaffolds. In tissue engineering, although a variety of biomaterials have been investigated, most of them are insufficient to be developed as ideal bioink. Bioink selection plays an important role in producing the stable 3D constructs with high biological compatibility. Current strategies include using cell-biomaterial based bioinks [3, 26].

The concept of cell-biomaterial based bioink is to provide a microenvironment for live cells grows, proliferate, occupy the space, and secrete their matrix before the scaffold is degraded. Cells are usually encapsulated into bioinks before printing to increase the cellular activity, and optimize their spatial distribution within the scaffold [2, 15]. The materials for bioinks should satisfy certain requirements: printability and biocompatibility. A variety of biomaterials including natural-derived and synthetic polymers are being investigated for 3D bioprinting. Among them, hydrogels are considered as attractive candidates [27, 28].

Hydrogels are hydrophilic polymeric networks that can mimic the physical and biochemical functions of native extracellular matrix. The plasticity and viscoelasticity of hydrogels allow the printing of a 3D construct with high shape fidelity [29, 30].

Many hydrogel bioinks have been developed, such as gelatin, collagen, chitosan, hyaluronic acid, for various types of tissue. However, the development of an ideal bioink is still in the early stage. The gelation mechanism based on physical, chemical or ionic crosslink has a great impact on the printability and long-term cell culture [31, 32].

Since most synthetic polymers are bio-inert and natural polymeric hydrogels exhibit poor mechanical properties, the bioinks fabricated from the combination of natural/synthetic polymers are more preferred [33-35].

2.3.1 Silk fibroin-based bioink

Silk fibroin (SF) has been reported to have unique mechanical strength and biocompatibility among fibrous proteins in biomedical applications. SF is extracted from silk cocoon in the form of aqueous solution and further fabricated into silk film, silk particle, silk scaffold, and silk hydrogel for both soft and hard tissue regeneration [7, 36]. In term of 3D bioprinting, SF's printability is hard to handle due to high molecular weight and low viscosity. There have been several strategies in improving SF printing processability, particularly, increasing its concentration, or adding other viscous additives [37, 38]. Among these, the combination of SF with polysaccharides such as gelatin, alginate, and collagen is effective for adjusting silk bioink's rheology [39]. Gelatin gains much attention for modulating SF printability and provides a bioactive environment for embedded cells. The weak mechanical properties of gelatin was supported by the incorporation of SF [40, 41]. SF-Collagen and SF-Alginate also showed the comprehensive physical properties in extruding printing, and maintained a long-term metabolic activity for bioink [41-43]. Consequently, SF based-multicomponent bioinks have been widely studied and put into practice for 3D tissue printing, especially bone and cartilage.

2.3.2 Hyaluronic acid-based bioink

Hyaluronic acid (HA) is one of the most abundant glycosaminoglycan in cartilage's extracellular matrix. Despite a wide range of its applications in tissue engineering and regenerative medicine, pure HA is unsuitable to produce bioink. HA's low viscosity implies no yield stress and no shape retention upon 3D printing [44]. Yet, several

attempts have been made to put HA bioink into bone and cartilage printing. By chemical modification or combination of HA with natural gelling polymers, it was shown that HA-based bioinks were potential rather than printing alone [45, 46]. A hydrogel consisting of hyaluronic acid (HA), hydroxyethyl acrylate (HEA) and gelatin-methacryloyl (GelMA) (HA-g-pHEA-GelMA) was studied as a bioprinting gel with bone cell loaded, and performed stable rheological properties, good shape maintenance, and high cell survival rate [47]. Photocrosslinked HA methacrylate (HAMA) bioink was investigated with osteogenic differentiation of the encapsulated mesenchymal stem cells (hMSCs) and showed limited shape fidelity [48]. In the same year, another versatile tyramine-modified hyaluronan (HA-Tyr) bioink was introduced for extruding printing, which was formulated by double crosslinking. The good printability and shape fidelity of HA-Tyr bioink were ensured by enzymatic crosslinking and green-light crosslinking, respectively [49]. The use of extracellular matrix component such as HA adds the capabilities of ideal bioink development. The combination of two or multiple biomaterials in bioink formulation makes it fulfill the certain requirements of 3D tissue printing including printability, post-printing construct maintenance, and biocompatibility. It is noted that very few cases that print a single biomaterial.

2.3.3 Alginate

Derived from brown algae, Alg contains β -D-mannuronate (M blocks) and α -L-glucuronate (G blocks) subunits bonded with 1, 4 linkage. Alg hydrogel possesses a long degradation time, and good mechanical properties, which is appropriate for long-term in vitro culture [50]. The mechanical properties of Alg is usually modulated by covalent binding among alginate G blocks via Ca^{2+} or other divalent cations to form 3D “egg box” structures [51]. Alg is also a popular material for bioink which could be prepared to print in CaCl_2 solution or combined with other materials such as agar, gelatin to adjust the viscosity. Alginate and agar were mixed to prevent the Barus effect in 3D printing [52]. This bioink was crosslinked by calcium ions, and the introduction of agar helped increase its viscosity to obtain a 3D structure after printing. Similarly, gelatin was added into Alg/gelatin bioink to optimize its flow behavior through the nozzle and post-printing crosslinked by CaCl_2 [23]. The use of

CaCl₂ as a building chamber can crosslink Alg-based material right away after extrusion, however, solution removal afterwards may result in low resolution. Clogging in the nozzle also happened when dipping the printing head in the solution during printing.



CHAPTER 3

RESEARCH METHODOLOGY

3.1 Materials

Hyaluronic acid sodium (molecular weight 1.6×10^6 Da) (53747), Sodium alginate (W201502), Lithium bromide (LiBr) (213225), ethylene diamine (753084), 1-hydroxybenzotriazole hydrate (HOBt) (54802), 1-ethyl-3-(3-dimethylaminopropyl) carbodiimide hydrochloride (EDC) (03450), sodium periodate (NaIO₄) (S1878), ethylene glycol (324558), and sodium chloride (NaCl) (S9888), dimethyl sulfoxide (DMSO) (D48418) were purchased from Sigma-Aldrich (St. Louis, MO, USA). HyClone Minimal Essential Medium (alpha MEM) used for cell culture was purchased from Cytiva (Logan, Utah, USA). High glucose DMEM (D777) was purchased from Sigma-Aldrich (St. Louis, MO, USA). Gibco™ HEPES (15630-080) and Gibco™ antibiotic-antimycotic (A5955), Gibco™ fetal bovine serum were purchased from ThermoFisher Scientific (Waltham, MA, USA). TrypLE™ Express Enzyme (12604021) and Invitrogen™ LIVE/DEAD® viability/cytotoxicity kit (L3224), PrestoBlue™ (P50200), Quant-iT™ Picogreen™ dsDNA Assay Kit (P7589) were purchased from ThermoFisher Scientific (MA, USA).

3.2 Synthesis of amine hyaluronic acid (HA-NH₂):

The 0.5 g of HA was dissolved in 100 mL deionized water (DI) to make a concentration of 5 mg/mL solution. A 30-molar excess of ethylene-diamine was added into the HA solution. The pH of the solution was adjusted to 6.5 by HCl, resulting in the reaction mixture. Next, EDC (0.8 g) and HOBt (0.7 g) were dissolved in 10 mL of DMSO in water (1: 1 v/v) and added dropwise to the reaction mixture. The HA reaction mixture was stirred for 24 hours at room temperature and dialyzed (molecular weight cut-off 14000 Da, Sigma-Aldrich, MO, USA) against DI water for 3 days with DI water changes every 8 hours [53]. The solution in dialysis bag was transferred into a sterile container and subjected to salting out by addition of NaCl to final concentration of 5% w/v. The white HA-NH₂ precipitation was collected in 70%

ethanol, re-dissolved in water, and then dialyzed for 3 days to remove NaCl. The final product was freeze-dried and stored at 4°C. All steps were prepared in a biosafety cabinet.

3.3 Synthesis of aldehyde-modified alginate (Alg-CHO):

Alg was dissolved in 100 mL of DI water to obtain a final concentration of 2% w/v. 5 mL of 0.5 M NaIO₄ was added to sodium alginate solution and stirred for 2 hours at room temperature in the dark. Ethylene glycol (1 ml) was used to quench the excess NaIO₄. The resulting solution was stirred for 2 hours and then dialyzed against DI water for 3 days with DI water changes every 8 hours. The solution in dialysis bag was transferred into sterile container, freeze-dried, and stored at 4°C. All steps were prepared in a biosafety cabinet.

3.4 Preparation of silk fibroin

The 4 g of degummed silk was dissolved in 16 mL of 9.3 M lithium bromide solution at 60 °C for 4 hours. Then, the resulting solution was collected and dialyzed against DI water for 3 days in biosafety cabinet. DI water was changed every 8 hours within 3 days. Subsequently, the dialyzed silk fibroin solution was centrifuged at 9000 rpm, 4 °C for 20 minutes twice to separate silk solution from debris. Silk fibroin (SF) concentration was determined by weighing the remaining solid after drying. The SF solution was adjusted a final concentration to 6 mg/mL in DI water [54].

3.5 Fabrication of the HA-Alg hydrogel

The dry products of HA-NH₂ and Alg-CHO were dissolved separately in 1xPBS to reach a concentration of 30 mg/mL and 20 mg/mL. The HA-Alg hydrogels were fabricated by thoroughly mixing HA-NH₂ and Alg-CHO solutions at various volume ratio of 2:8, 3:7, 4:6, 5:5, 6:4, 7:3, 8:2 at room temperature (Table 1).

3.6 Fabrication of HA-Alg-SF hydrogel

The HA-Alg-SF hydrogel was prepared as the following steps. Firstly, HA-NH₂ was dissolved in PBS and added with SF solution to make a final concentration of 30 mg/mL HA-NH₂ and 2 mg/mL SF. Secondly, Alg-CHO was dissolved in PBS to

result in a 20 mg/mL solution. HA-NH₂/SF and Alg-CHO solutions were mixed following the optimal ratio investigated from previous HA-Alg hydrogel. Optimal ratio of HA-Alg hydrogel was determined based on gelation and degradation test, which allows the injectability and appropriate degradation time for cell culture.

3.7 Characterization of HA-Alg and HA-Alg-SF hydrogel

3.7.1 Nuclear Magnetic Resonance (NMR) analysis

The pure HA, Alg, freeze-dried HA-NH₂, and freeze-dried Alg-CHO were dissolved in deuterium oxide (D₂O) and transferred to 5 mm NMR sample tubes. The NMR spectra were recorded by Bruker AVANCE III 500 MHz spectrometer (Billerica, MA, USA). One dimensional ¹H and ¹³C resonances were obtained and analyzed by Mnova (Mestrelab, ver.14.1).

3.7.2 Fourier transform infrared spectroscopy (FTIR) analysis

The freeze-dried samples were ground with KBr powder. FTIR spectra were obtained in the range of wavenumber from 4000 to 500 cm⁻¹. The spectrum was averaged over 64 scans with 4.0 cm⁻¹ resolutions (Perkin Elmer, Spectrum One, USA). The spectra were documented and analyzed by Origin (Origin Lab, ver.2021).

3.7.3 Swelling and degradation analysis

The initial wet weight (W₀) of hydrogels (n=3) was recorded. Then hydrogels were submerged in 1xPBS solution (pH 7.4) at 37 °C for 60 days. Hydrogels were removed from PBS solution, recorded wet weight (W_t) at different time points to calculate percentage of swelling and degradation weight loss, W_d (%), as described in equation below.

$$W_d (\%) = (W_t - W_0) / W_0 \times 100$$

3.7.4 Rheological properties of hydrogels

Rheological measurements of hydrogels were performed with a rheometer (HAAKE MARS III, ThermoScientific, USA) equipped with parallel plates set in oscillatory mode at room temperature. Strain sweep experiment was conducted over a range of 0.1-100%, at 1 Hz to determine the linear viscoelasticity region (LVER) of the

hydrogels, which indicated the range of strain rate applied on the samples. Then, the dependence/independence of elastic modulus (G') and viscous modulus (G'') over a range of oscillation frequencies (0.01 to 100 Hz) was acquired at the defined strain rate. Time sweep experiment was performed to determine the gelation time at 1 Hz. The viscosity of hydrogels over a shear rate (0.001 to 1000 s^{-1}) was recorded.

3.7.5 Mechanical Assessment of hydrogels

Mechanical properties of hydrogels ($n=3$) was measured by a Hounsfield electronic universal testing machine (Hounsfield HT, USA) at room temperature. The hydrogels 13 mm in diameter and 10 mm in thickness were placed into the testing machine with a constant velocity of 10 mm/min in compressive mode. All hydrogel samples were compressed to 50% height of their original cylindrical shape.

3.7.6 Printability of HA-Alg (5:5) and HA-Alg-SF

The Alg-CHO was mixed with an equal volume of HA-NH₂, transferred into a syringe and printed through 18G needles (outer diameter: 1.27 mm, inner diameter: 0.838 mm) using a custom-made 3D printer equipped with a screw-driven extruder (Enterprise 2.0) (Fig. 7A). The printed patterns were designed by Blender software (Blender, ver.9.3 LTS) and the G-codes files were generated using a slicing software (Simplify3D ver.4.0). The printing condition was maintained at 37 °C with speed of 60 mm/min. To investigate cell viability in 3D printed constructs, hMSCs (10^6 cells/mL) were mixed with Alg-CHO, combined with an equal volume of HA-NH₂ or HA-SF solution and transferred into a syringe. The cell/hydrogel was printed through 18G needle into 2 layers of grid patterns (total dimension was 1.5 mm x 1.5 mm x 0.2 mm) on a petri dish. Cell viability was assessed by LIVE/DEAD® Kit staining and observed under fluorescence microscope (Nikon Eclipse Ti, USA) 1 day post-printing.

3.7.7 Cytotoxicity and biocompatibility evaluation of hydrogels

3.7.7.1 Sample sterilization

Chemical modification of HA and Alg was conducted in a biosafety cabinet. All chemicals and reagents were filtered before use. The lyophilized HA-NH₂ and Alg-CHO were UV sterilized for 20 mins in biosafety cabinet prior to cell culture experiment.

3.7.7.2 Cell culture and cell encapsulation in hydrogels

Human mesenchymal stem cells (hMSCs) (Lonza, Walkersville, MD) were maintained in hMSC medium (Alpha Modified Eagle's Medium (α MEM) supplemented with 5% (v/v) Fetal Bovine Serum (FBS), 1% (v/v) GlutaMAX, 1% (v/v) HEPES buffer, 1 ng/mL of fibroblast growth factor-basic (bFGF) (Invitrogen), and 1% (v/v) antibiotic-antimycotic solution) at 37 °C, 5% CO₂. The medium was changed every 3 days. Subculturing was performed using 0.25% Trypsin-EDTA when cells reached 80% confluency. For cell encapsulation, the 50 μ L of HA-Alg or HA-Alg-SF solution was mixed with 5 x 10⁴ cells (1 x 10⁶ cells/mL), transferred into 6 mm \times 8 mm cloning rings (Pyrex, Sigma Aldrich) and incubated at 37°C, 5% CO₂ for 2 hours. Then, cell/hydrogel constructs were pushed out from cloning rings and cultured in hMSC medium.

3.7.7.3 Live/dead assay

According to ISO standard 10993-5:2009, hydrogels were directly assessed cytotoxicity by LIVE/DEAD® Kit. The constructs (n=3) were incubated in Calcein AM/EthD-1 for 30 minutes in the dark as described in the manufacture's instruction. The hydrogel constructs were visualized using inverted fluorescence microscope (Nikon, Eclipse Ti) to determined living (green) and dead (red) cells on day 1, 3 and 7 post-encapsulation.

3.7.7.4 Quant-iT™ Picogreen™ dsDNA Assay

The constructs (n = 3) were removed from culture medium, minced and digested in 1mL of 1mg/mL proteinase K (P2308, Sigma-Aldrich, MO, USA) containing 20 μ L papain solution (P4762, Sigma-Aldrich, MO, USA) Then, DNA content was measured using Quant-iT™ Picogreen™ dsDNA Assay Kit according to standard

protocol. Samples were measured at λ_{ex} 480 nm and λ_{em} 530 nm using a microplate reader (Varioskan Lux, Thermo Scientific, USA). Fibrin hydrogel was used as control [55].

3.7.7.5 PrestoBlue™ assay

The constructs (n=3) on day 1, 3 and 7 post-encapsulation were incubated in 1 mL of 1x PrestoBlue™ diluted in medium, following the manufacture's instruction. The constructs were incubated at 37 °C, 5% CO₂ for 3 hours. Then, the incubated medium was taken out and transferred to a 96 well-plate. The fluorescence was measured at λ_{ex} 560 nm and λ_{em} 590 nm using a microplate reader (Varioskan Lux, Thermo Scientific, USA). Fibrin hydrogel was used as control [55]. Blanks wells were HA-Alg, HA-Alg-SF, and fibrin hydrogels without cell encapsulation.

3.7.7.6 Ki-67 staining

1-week cultured constructs were fixed in 4% formalin for 2 hours at room temperature, then transferred into 30% sucrose at 4°C overnight before embedding in cryogel (FCS 22 Clear, Leica). The constructs were sectioned to 5 µm thick. Sections were pre-treated with proteinase K buffer for antigen retrieval, permeabilized with 0.1% v/v Triton-X100. After that, the sections were incubated with normal blocking serum, rabbit anti-human IgG Ki67 (ab15580, Abcam, UK) at 1:200 dilution, biotinylated secondary antibody, avidin-biotin-peroxidase (Vectastain Elite ABC kit, Vector Laboratories), and ImmPACT® DAB Peroxidase Substrate (HRP, Vector Laboratories), followed the guideline.

3.7.8 Cartilage tissue development

3.7.8.1 Chondrogenic differentiation

The cells/hydrogel constructs (seeding density of 1×10^6 cells/mL) were culture in chondrogenic medium (DMEM supplemented with 1% (v/v) ITS, 1% (v/v) HEPES buffer, 0.1% (v/v) L-proline, 0.1% (v/v) Ascorbic acid, 0.4 µg/mL of dexamethasone, 5 ng/mL of TGF-β3, and 1% (v/v) anti/anti) for 2 and 4 weeks with every 3 day medium change.

3.7.8.2 Immunofluorescent staining

At 2-week and 4-week chondrogenic differentiation of hMSC, the constructs were fixed in 4% formalin for 2 hours at room temperature, then transferred into 30% sucrose at 4°C overnight before embedding in cryogel (FCS 22 Clear, Leica). The constructs were sectioned on transverse plane to 5 µm thick. The sections were pre-treated with proteinase K buffer for antigen retrieval for 20 minutes, rinsed with PBS, and incubated with blocking serum (Vectastain Elite ABC kit, Burlingame, CA) for 30 minutes at room temperature, and incubated with 1: 200 rabbit polyclonal to collagen type II antibody (ab34712, Abcam, UK) for 1 hour. The sections were washed, and incubated with anti-rabbit secondary antibody conjugated with Texas Red (ab7088, Abcam, UK) for 1 hour at room temperature in the dark. Negative control samples were hydrogel sections without primary antibody incubation. All samples were counterstained with DAPI- aqueous Fluoroshield (ab1041239, Abcam, UK). The sections were visualized under an inverted fluorescence microscope (Nikon, Eclipse Ti, USA).

3.8. Statistical analysis

Statistical analysis was performed using Stata. Data were expressed as average \pm standard deviation (SD) of $n = 3$ unless otherwise specify. The differences in cell proliferation in PrestoBlue™ and Quant-iT™ Picogreen™ dsDNA Assay were evaluated using one-way ANOVA followed by Tukey's post-test with $\alpha = 0.05$ to consider statistical significance.

CHAPTER 4

DATA ANALYSIS AND INTERPRETATION

4.1 NMR analysis of HA-NH₂ and Alg-CHO

Figure 1 shows the spectra of HA and modified HA-NH₂, the signals from 3.43 to 3.87 ppm were assigned to the protons on the sugar rings [56, 57]. The methyl (-CH₃) protons of the N-acetyl group of HA and HA-NH₂ showed a signal at 2.06 ppm (label a). In the spectrum of HA-NH₂, the presence of conjugated ethylenediamine was confirmed by the proton signals at 3.2 ppm (label b) and 2.93 ppm (label c) [58]. The new signals at 3.37 ppm and 3.94 ppm, indicating the chemical shift of protons in the sugar rings of HA-NH₂ after conjugating with primary amines.

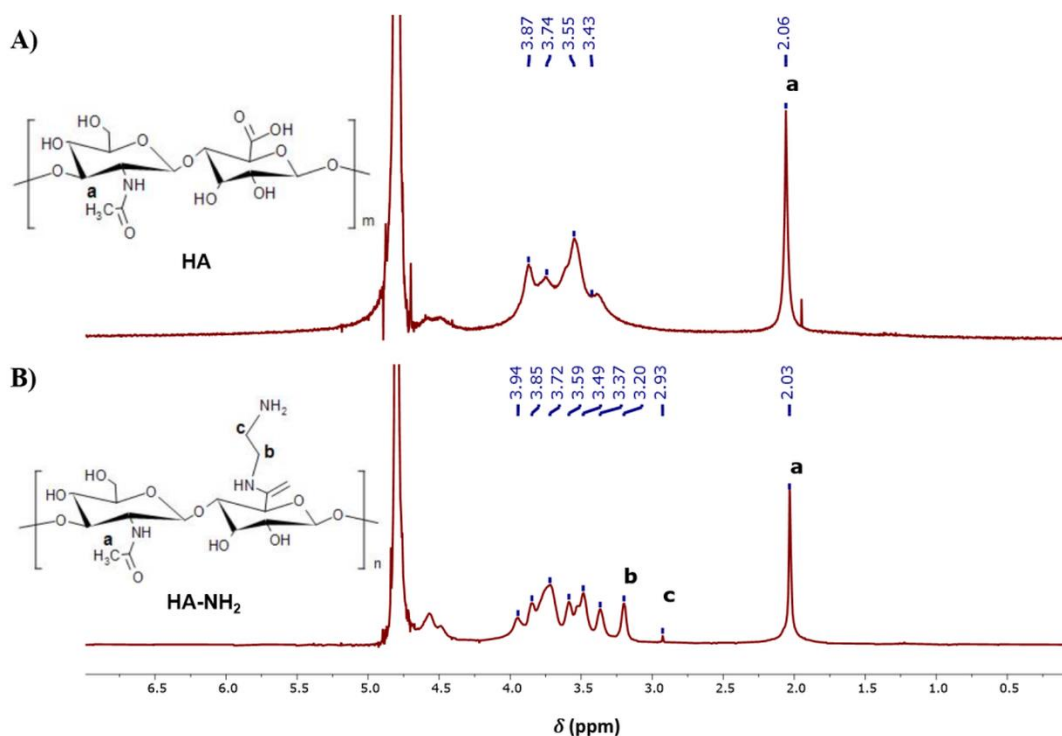


Figure 2. ¹H-NMR spectra of pure HA and modified HA-NH₂.

The ¹H NMR spectra of Alg and Alg-CHO were showed in Figure 3B and the signals at 5.06, 4.66, and 4.48 ppm corresponding to the position of G1, M1, 5 and G5 in the Alg backbone [59, 60]. After modification, oxidized alginate had the additional peaks at 5.55 and 5.74 ppm which corresponded to hemiacetalic protons formed from the

reaction of aldehyde with neighboring hydroxyl groups. The peaks of hemiacetalic protons in the Alg-CHO spectrum can confirm the successful modification of Alg with aldehyde groups. For ^{13}C NMR spectra in Figure 3C, Alg and Alg-CHO showed the signals corresponding to G blocks (G1, G2, G3, G4 and G5) and M blocks (M1, M4 and M5) in their sugar rings [61]. Comparing with the unmodified Alg, ^{13}C NMR spectrum of oxidized alginate had the new signals at 95.09 ppm and 92.73 ppm demonstrating the hemiacetalic carbons. The finding of hemiacetalic protons instead of aldehyde protons in oxidized alginate could be explained by the neutral reaction between generated aldehyde groups with the nearby hydroxyl groups in its polymer chain, and this reaction can be reversible in aqueous acid environment (Figure 3A) [5].

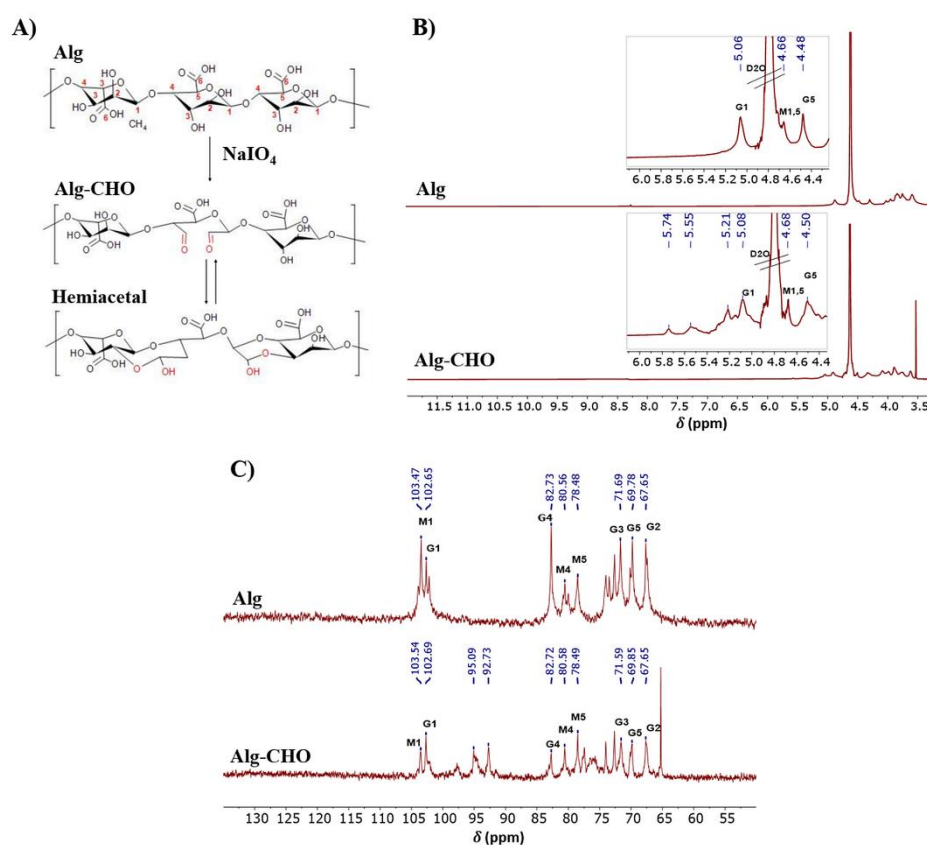


Figure 3. A) Oxidation of alginate by sodium periodate and the formation of intermolecular hemiacetal, B) ^1H -NMR spectra of pure Alg and modified Alg-CHO, C) ^{13}C -NMR spectra of pure Alg and modified Alg-CHO.

4.2 FTIR analysis of HA-NH₂, Alg-CHO and HA-Alg hydrogels

In the FTIR spectrum of HA-NH₂, the new peak at 3123 cm⁻¹ was observed which indicated the presence of N-H stretching in amine salt after chemical modification. The primary amines (-NH₂) in HA-NH₂ were confirmed by the peak of 1552 cm⁻¹ (Figure 4A) [62]. For Alg-CHO, the peak of aldehyde groups (-CHO) was observed at 1721 cm⁻¹ (Figure 4A), which corresponded with NMR analysis [63]. Gelation of HA-Alg hydrogel occurred as a result of imine formation (C=N) between -CHO and -NH₂ groups, as demonstrated by peak at 1636 cm⁻¹ (Figure 4B) [64].

For HA-Alg-SF hydrogel, peak of imine at 1636 cm⁻¹ was also observed. Incorporation of SF into HA-Alg-SF hydrogel presented a shifted FTIR spectrum in the 3600-3000 cm⁻¹ region, indicating the free amine groups on SF did not react with Alg-CHO (Figure 4B). The large amount of non-primary amines on SF cannot induce gelation after mixing SF with Alg-CHO [8]. The crosslinking system was mainly based on Schiff base reaction between Alg-CHO and HA-NH₂.

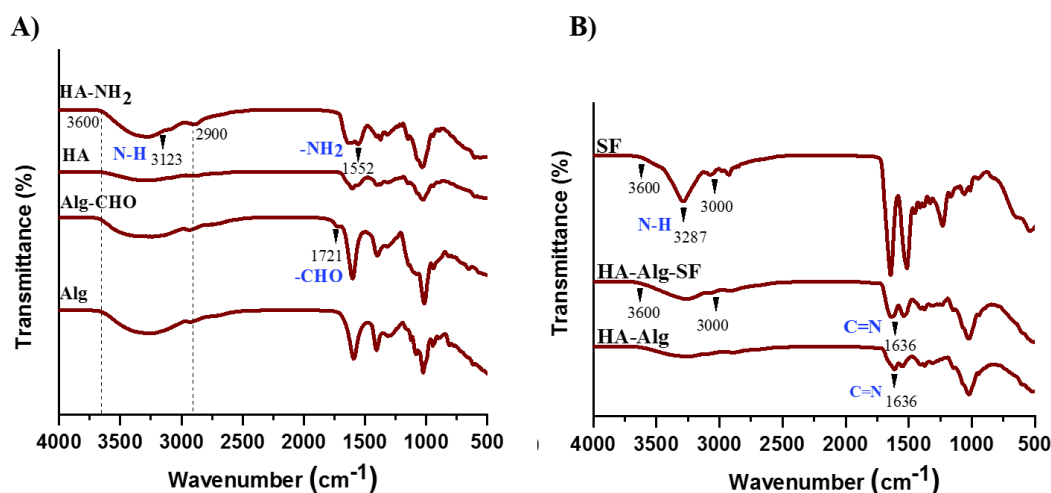


Figure 4. FTIR analysis of A) HA, HA-NH₂, Alg, Alg-CHO, and B) extracted SF, HA-Alg (5:5), HA-Alg-SF hydrogels.

4.3 Gelation of HA-Alg at varied volume ratio and HA-Alg-SF.

After modification, HA-NH₂ and Alg-CHO were fabricated into HA-Alg hydrogels with varied volume ratio of 2 : 8, 3 : 7, 4 : 6, 5 : 5, 7 : 3, 6 : 4 and 8 : 2 according to

Table 1. The gelation of HA-Alg hydrogels was monitored at room temperature. There were three volume ratios of HA-NH₂ and Alg-CHO (5:5, 6:4, 7:3) can perform gelation. The morphology and injectability of HA-Alg (5:5, 6:4, 7:3) through syringe needles were depicted in Figure 4. Gelation between HA-NH₂ and Alg-CHO with equal volume (5:5) formed a more rigid hydrogel comparing with the others. The volume ratio of HA-NH₂ and Alg-CHO at 5:5 was chosen for SF loading (Figure 5).

Table 1 . Formulation of HA-Alg hydrogel at varied volume ratio.

Volume ratio	HA-NH ₂ (μL)	Alg-CHO (μL)	Gelation
2:8	40	160	X
3:7	60	140	X
4:6	80	120	X
5:5	100	100	O
6:4	120	80	O
7:3	140	60	O
8:2	160	40	X

(O: form gel, X: do not form gel)

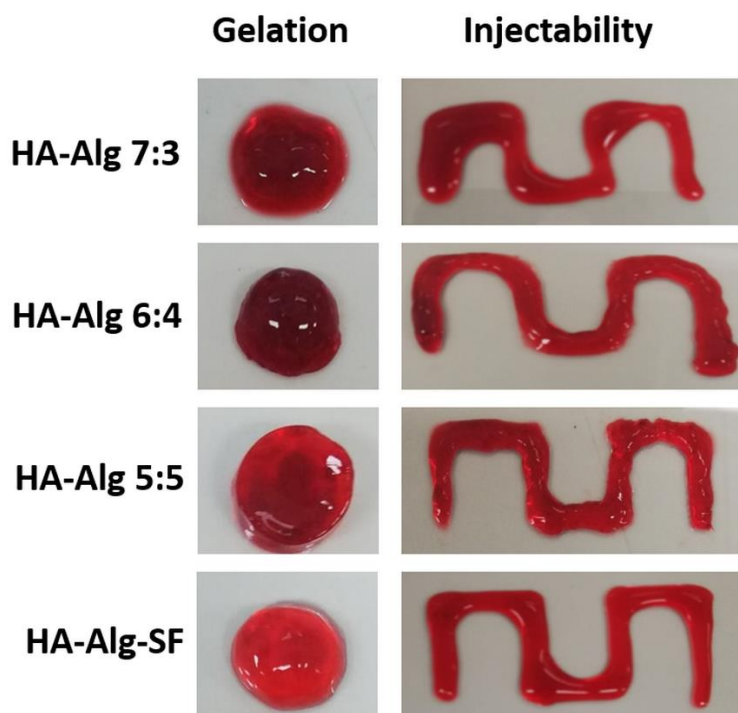


Figure 5. HA-Alg hydrogel at different volume ratios and HA-Alg-SF hydrogel made from HA-Alg (5:5).

4.4 Swelling and degradation behavior of hydrogels

In vitro swelling and degradation of HA-Alg at different volume ratios and HA-Alg-SF were demonstrated in Figure 6 and Table 2. It was noticed that the change in volume ratio between HA-NH₂ and Alg-CHO resulted in different swelling and degradation of HA-Alg hydrogels in PBS medium (pH=7.4).

In particular, the HA-Alg (7:3) showed its swelling in day 5 and day 10 which was $4.8 \pm 2.5\%$ and $8.6 \pm 2.1\%$, respectively. This formulation accompanied with the fasted degradation after 35 days comparing with the others.

The HA-Alg (6:4) expressed an insignificant swelling during incubation, and its degradation was recorded with $89.4 \pm 5.3\%$ only after 40 days.

The HA-Alg (5:5) possessed a stability during 35 days and degraded slowly until reaching $38.3 \pm 14.9\%$ of weight loss on day 60.

HA-Alg-SF hydrogel swelling and degradation were also investigated when SF was added into HA-Alg (5:5) network. HA-Alg-SF hydrogel was swollen approximately

by $4.4 \pm 1.9 \%$ and $8.7 \pm 2.4 \%$ on day 15 and 20. After that, this hydrogel started to degrade from day 25 and by $82.8 \pm 0.8 \%$ on day 60. This result revealed that the addition of SF in the HA-Alg system could not slow down the degradation of hydrogel but increased the swelling of HA-Alg-SF comparing with HA-Alg (5:5).

The variation of volume ratio between HA-NH₂ and Alg-CHO resulted in varied crosslinked degree of hydrogel network. Therefore, when increasing the ratio of HA-NH₂ in the formulation (5:5, 6:4, 7:3), the crosslinked polymer was less rigid, absorbed more water and degraded faster. The swelling and degradation behavior of HA-Alg-SF comparing with HA-Alg (5:5) inferred that SF did not significantly improve hydrogel mechanical properties.

Table 2. Weight difference (%) of hydrogels in PBS for 60 days.

Day	Weight difference (%)			
	HA-Alg (7:3)	HA-Alg (6:4)	HA-Alg (5:5)	HA-Alg-SF
1	0.0	0.0	0.0	0.0
5	4.8 ± 2.5	2.5 ± 2.5	0.3 ± 7.8	2.6 ± 1.7
10	8.6 ± 2.1	3.8 ± 2.4	0.7 ± 6.9	4.3 ± 1.6
15	5.6 ± 2.3	-5.1 ± 2.6	0.7 ± 7.4	4.4 ± 1.9
20	-17.2 ± 1.6	-19.9 ± 3.7	0.8 ± 7.6	8.7 ± 2.4
25	-39.3 ± 1.4	-38.3 ± 4.1	0.9 ± 7.7	2.1 ± 1.04
30	-63.1 ± 3.2	-56.3 ± 4.9	1.2 ± 7.3	-7.1 ± 1.3
35	-77.6 ± 3.4	-72.3 ± 5.8	0.8 ± 7.5	-13.4 ± 1.1
40	-95.4 ± 8.0	-89.4 ± 5.3	1.1 ± 8.3	-27.9 ± 3.0
45		-96.7 ± 5.6	-1.4 ± 8.8	-50.9 ± 2.4
50			-6.8 ± 9.8	-56.8 ± 3.1
55			-24.9 ± 11.9	-77.2 ± 0.6
60			-38.3 ± 14.9	-82.8 ± 0.8

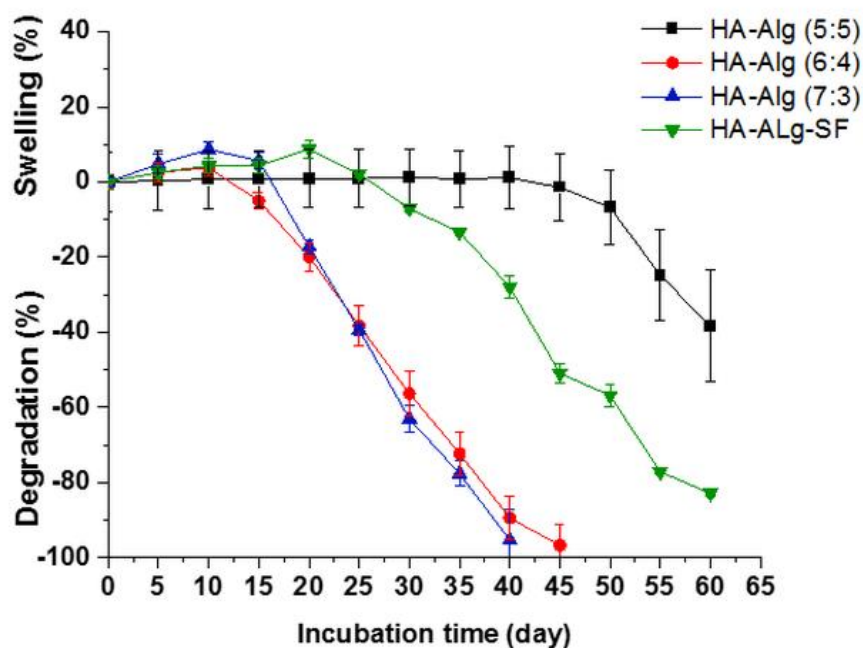


Figure 6. Swelling and degradation profiles of HA-Alg and HA-Alg-SF hydrogels (mean \pm SD).

4.5 3D Printing of HA-Ag (5:5) and HA-Alg-SF bioinks

HA-Alg and HA-Alg-SF hydrogels were used as bioink and printed by a laboratory custom-made 3D printer (Enterprise 2.0) (Figure 7A). Figure 7B shows the printability and 3D construct formation of HA-Alg (5:5) bioink after printing.

Both HA-Alg (5:5) and HA-Alg-SF bioinks were encapsulated with hMSCs and printed as a gridline matrix with 2 layers (1.5 mm x 1.5 mm x 0.2 mm). After 1-day culture, the encapsulated cells were stained with LIVE/DEAD® Kit. Crowded population of green dots accounted for high cell viability. It also showed that cells distributed evenly through the constructs after printing (Figure 7C).

In conclusion, HA-Alg and HA-Alg-SF hydrogel were printable and biocompatible for cell encapsulation.

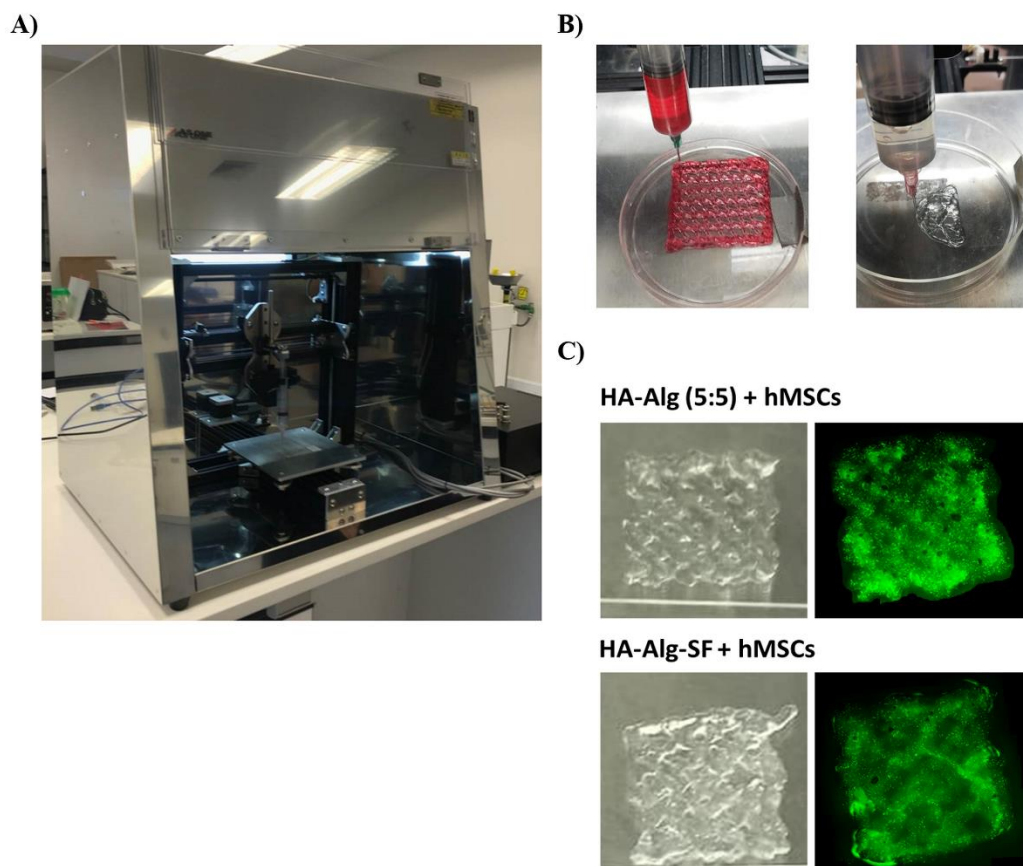


Figure 7. A) Custom-made 3D printer (Enterprise 2.0) B) 3D printing of HA-Alg (5:5), C) Printing of HA-Alg (5:5) and HA-Alg-SF hydrogels with hMSCs loading

4.6 Compressive strength of hydrogels

From previous experiments, HA-Alg (5:5) and HA-Alg-SF hydrogels were considered as bioinks for 3D printing. Thereby, the information of mechanical properties of HA-Alg (5:5) and HA-Alg-SF were examined.

Figure 8 shows the compression stress-strain curves and the mechanical properties of HA-Alg (5:5) and HA-Alg-SF hydrogels. Under compressive loading, both HA-Alg (5:5) and HA-Alg-SF hydrogels displayed a gradual increase in stiffness and could withstand to 50% of compressive loading. After that, the hydrogels recovered to their original shape (Figure 8A). The compressive strength of HA-Alg (5:5) and HA-Alg-SF hydrogels were 11.44 ± 1.80 kPa and 10.61 ± 0.36 kPa at the strain of 50% (Figure 8B). There was no significant difference in elastic modulus between HA-Alg and HA-

Alg-SF hydrogels with 22.5 ± 1.36 kPa vs. 20.31 ± 1.36 kPa at 50% strain, respectively, ($p > 0.05$) (Figure 8C).

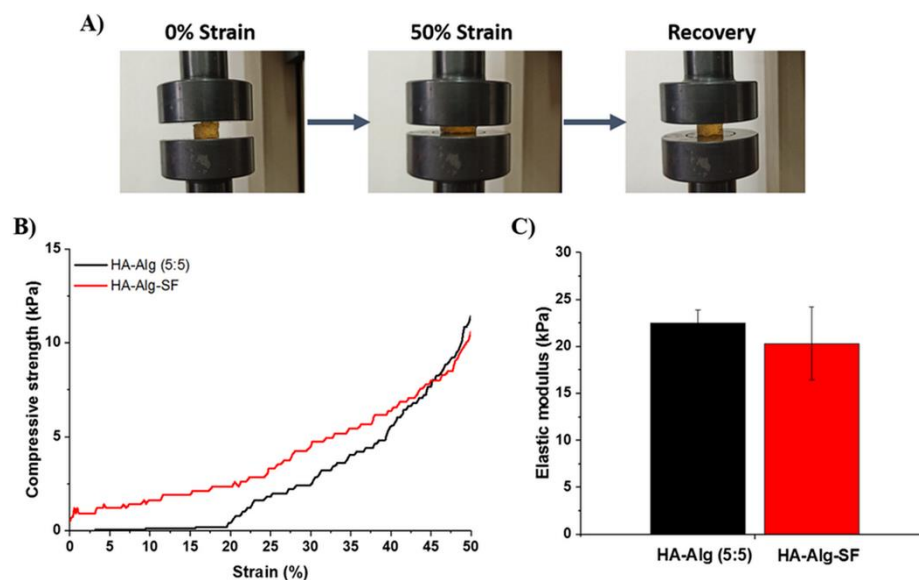


Figure 8. Compressive strength of hydrogels A) Recovery ability of HA-Alg (5:5) after compression, B) Typical compressive stress-strain curve of HA-Alg (5:5) and HA-Alg-SF hydrogels, C) The elastic modulus of HA-Alg and HA-Alg-SF hydrogels.

4.7 Rheological properties

The dynamic rheological properties of HA-Alg (5:5) and HA-Alg-SF hydrogels were characterized by strain sweep, frequency sweep, time sweep, and its shear-thinning behavior.

Initially, strain sweep test was used to check the linear viscoelasticity region of the hydrogel, which indicates the range of strain amplitude that do not destroy the hydrogel structure. Here, a strain sweep from 0.1-100% was conducted at frequency of 1 Hz on fully formed HA-Alg (5:5) or HA-Alg-SF hydrogels. The storage (G') and loss (G'') moduli were found beyond 100% for both HA-Alg (5:5) and HA-Alg-SF hydrogels (Figure 9A). This suggests that the HA-Alg and HA-Alg-SF were stretchable and had a relatively large deformation.

Then, frequency sweeps from 0.01 to 100 Hz were carried out at 1% strain, corresponding with the determined LVE strain amplitude (Figure 9B). The crossover points between G' and G'' for HA-Alg (5:5) and HA-Alg-SF were 78 Hz and 61 Hz, respectively. Below these points, the elastic behavior dominated the properties of the

hydrogels ($G' > G''$). On the other hand, exceeding the crossover point, both hydrogels showed a more fluid-like behavior at high frequency, which means the high frequency interrupted the hydrogel structure. This experiment indicated the dependence of G' and G'' on frequency.

Time sweep of HA-Alg (5:5) and HA-Alg-SF hydrogels was expected to provide information of gelation time. Time sweep was conducted at room temperature for 30 minutes. Basically, the gelation of a sample is observed by the crossover of G' and G'' . Before the gelation, G'' is greater than G' which shows the liquid behavior. When the gelation occurs, G' is equal to G'' and ultimately exceeds G'' value according to time. Figure 9C shows that there were no gelation points of HA-Alg and HA-Alg-SF, however, G' was greater than G'' for both hydrogels indicating the elastic behavior of crosslinked hydrogels. The absence of gelation point could be explained by the quick reaction of HA-NH₂ and Alg-CHO before loading into the plate geometry of rheometer.

Figure 9D demonstrates the viscosity of HA-Alg (5:5) and HA-Alg-SF hydrogels against the shear rate. The peak in viscosity represents the point where the hydrogels begin to flow. HA-Alg (5:5) and HA-Alg-SF hydrogels had viscosity peaks at 30.4 Pa.s and 12.6 Pa.s, respectively. Prior to viscosity peak, the hydrogels were undergoing elastic deformation. Correspondingly, at the shear rate higher than 9.1 s⁻¹ and 6.6 s⁻¹ for HA-Alg (5:5) and HA-Alg-SF hydrogels, a significant decrease in viscosity was observed, indicating their remarkable shear-thinning behavior. The viscosity of HA-Alg (5:5) was 0.12 Pa.s, and HA-Alg-SF was 0.13 Pa.s at the shear rate of 1000 s⁻¹. The shear-thinning property of these hydrogels indicates that they readily flow through the nozzle during printing process but can retain the gel structure after extruding [65]. An extruded-3D printer is basically able to print a highly viscous bioink (6×10^7 mPa.s) [66], therefore, the viscosity of HA-Alg (5:5) and HA-Alg-SF hydrogels compromised the printability.

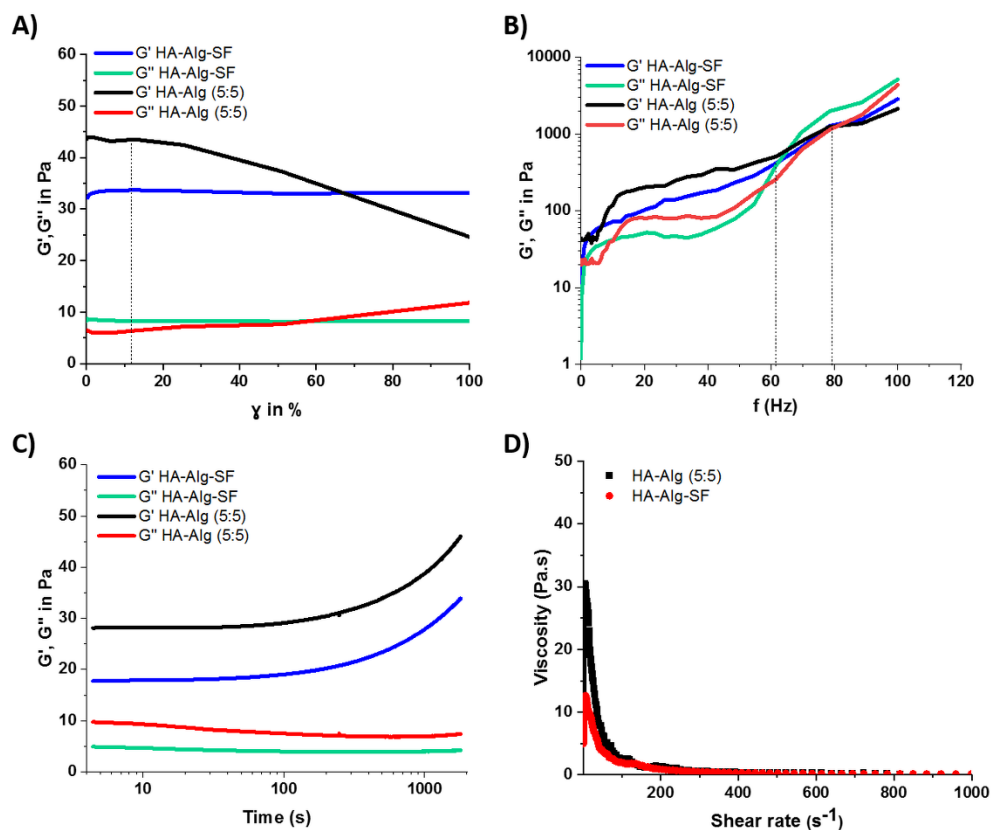


Figure 9. Rheological analysis of HA-Alg and HA-Alg-SF hydrogel a) Strain sweep, B) Frequency sweep, C) Time sweep, D) Shear-thinning properties of HA-Alg (5:5) and HA-Alg-SF.

4.8 In vitro cytocompatibility of HA-Alg and HA-Alg-SF hydrogels

4.8.1 In vitro live/dead

The cell viability and their distribution in HA-Alg (5:5) and HA-Alg-SF hydrogels were observed under fluorescent microscope and depicted in Figure 10. After 1, 3, and 7 days, the live cells in both 3D HA-Alg (5:5) and HA-Alg-SF hydrogels are shown as a crowded population (green dots). A minority of dead cells indicated by red dots was also observed during culture period. HA-Alg (5:5) and HA-Alg-SF hydrogels demonstrated its compatibility with the number of live cells remarkably outweighing dead cells. The results also revealed that there was no difference in cell viability between HA-Alg (5:5) and HA-Alg-SF hydrogels, and these hydrogels can provide an extracellular matrix for cell encapsulation.

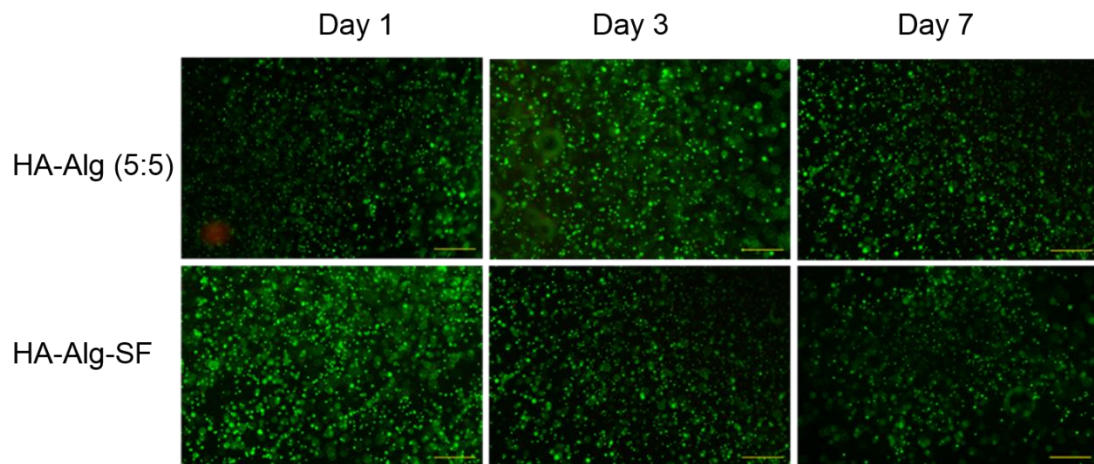


Figure 10. Live/Dead staining of hMSCs encapsulated in 3D HA-Alg (5:5) and HA-Alg-SF hydrogels in 1, 3, 7 days, (scale bars=500 μm).

4.8.2 Quant-iT™ Picogreen™ dsDNA Assay

Quant-iT™ Picogreen™ dsDNA Assay was used to determine cell proliferation of hMSCs in the 3D structure of HA-Alg and HA-Alg-SF in 1, 3, and 7 days. Fibrin hydrogel [55], which was a gold standard hydrogel, was used as control. Figure 11B shows that during 7 days of culture, the DNA amount (ng/sample) of each sample slightly increased. After the first day, HA-Alg hydrogel presented a significantly higher DNA amount than HA-Alg-SF, whereas no difference when comparing HA-Alg/Fibrin hydrogels, and HA-Alg-SF/ Fibrin. On day 3, HA-Alg hydrogel accounted for a significantly higher DNA quantity than both HA-Alg-SF and Fibrin hydrogel. On day 7, there was no difference between HA-Alg (5:5) and Fibrin while both these hydrogels presented higher DNA amount than HA-Alg-SF.

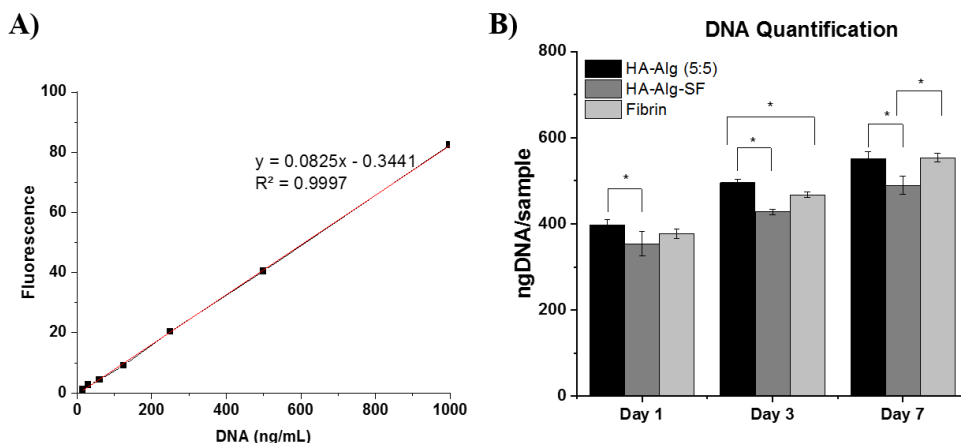


Figure 11. Quant-iT™ Picogreen™ dsDNA Assay. A) Standard curve, B) DNA amount detected from HA-Alg (5:5) and HA-Alg-SF hydrogels comparing with Fibrin.

4.8.3 PrestoBlue™ assay

PrestoBlue™ assay were also employed to quantitatively examine the cell viability and proliferation of hMSCs encapsulated in HA-Alg and HA-Alg-SF hydrogels. In PrestoBlue™ assay, absorbance values were used as the measurement of cell viability with high level of resofurin reflecting high level of cell metabolism [67]. As presented in Figure 12, the relatively fluorescent units which corresponds to the viability of hMSCs encapsulated in HA-Alg and HA-Alg-SF hydrogels in 1, 3, and 7 days. HA-Alg hydrogel had greater cell viability than HA-Alg-SF and Fibrin hydrogel. On the other hand, HA-Alg-SF hydrogels has lower cell viability than Fibrin hydrogel. All three samples had the increase in fluorescence unit through 7 days of culture, indicating the proliferation of encapsulated hMSCs in 3D hydrogels.

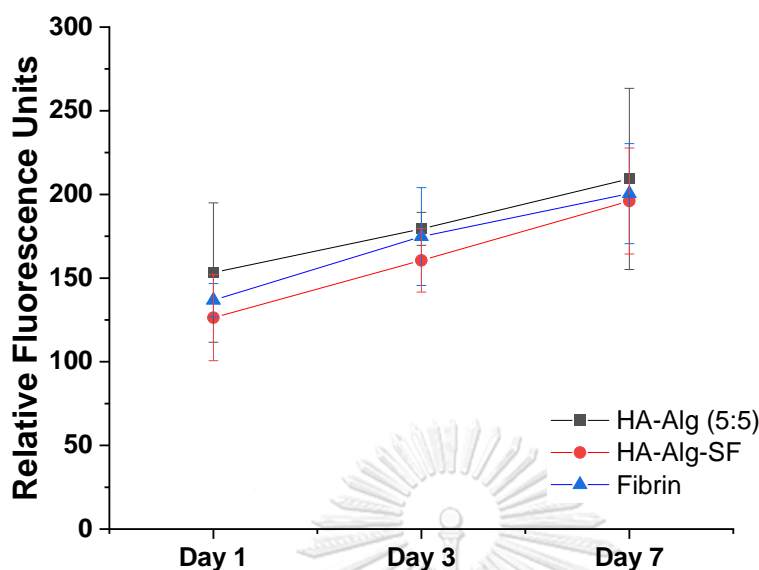


Figure 12. PrestoBlue™ assay in cell proliferation of HA-Alg (5:5), HA-Alg-SF, and Fibrin hydrogels after 1, 3, 7 days.

4.8.4 Immunochemical staining of Ki-67

Together with the assays of cell proliferation using Quant-iT™ Picogreen™ and PrestoBlue™, the HA-Alg (5:5) and HA-Alg-SF hydrogels encapsulated hMSCs after 7 days were sectioned and stained with anti Ki-67 to figure out the active cells. Ki-67 is a nuclear protein that is only present in the cell interphase (G₁, S, G₂) and mitosis [68]. Figure 13 shows the brown dots corresponding to Ki-67 protein in the cell nuclei, demonstrating that cells were active in hydrogel matrix after 7-day culture. This results also confirms data in DNA assay and PrestoBlue™ assays, in which cells proliferated after encapsulating into 3D HA-Alg (5:5) and HA-Alg-SF.

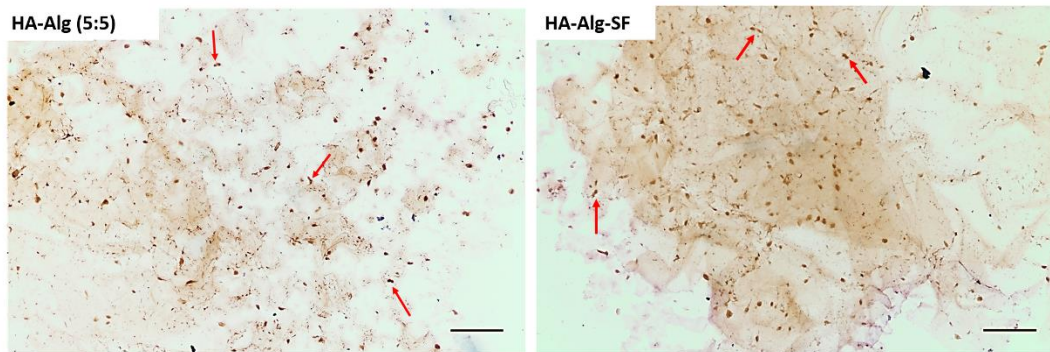


Figure 13. Immunohistochemical staining of Ki67 in HA-Alg (5:5) and HA-Alg-SF hydrogels after 7 days of cell culture, (scale bars=200 μ m).

4.9 Cell differentiation in HA-Alg (5:5) and HA-Alg-SF hydrogels

hMSCs were encapsulated into HA-Alg (5:5) and HA-Alg-SG hydrogels and added with chondrogenic medium, which consisted of ascorbic acid, dexamethasone, TGF- β 3 growth factor. The 3D hydrogel constructs encapsulated hMSCs were pictured in Figure 14A. Initially, both HA-Alg (5:5) and HA-Alg-SF hydrogels were transparent, while HA-Alg-SF had a light yellow color due to SF addition (week 0). Through culture period, there appeared white opaque surrounding both hydrogel constructs. This suggested the matrix secretion of differentiated hMSCs in the hydrogels. The chondrogenic differentiation of hMSCs was assessed using antibody of type II Collagen. Data from Figure 14B show that hMSCs in HA-Alg and HA-Alg-SF matrix demonstrated a secretion of type II Collagen after 2 weeks, and a significant greater type II Collagen content after 4 weeks (red). The increase in Col-II secretion was similar in both HA-Alg and HA-Alg-SF hydrogels. Negative controls were HA-Alg and HA-Alg-SF encapsulated hMSCs after 4 weeks, which were immunostained without primary antibody and mounted with DAPI. The control samples were depicted with blue dots, indicating the nucleus of cells on the gel matrix and no red area was recorded.

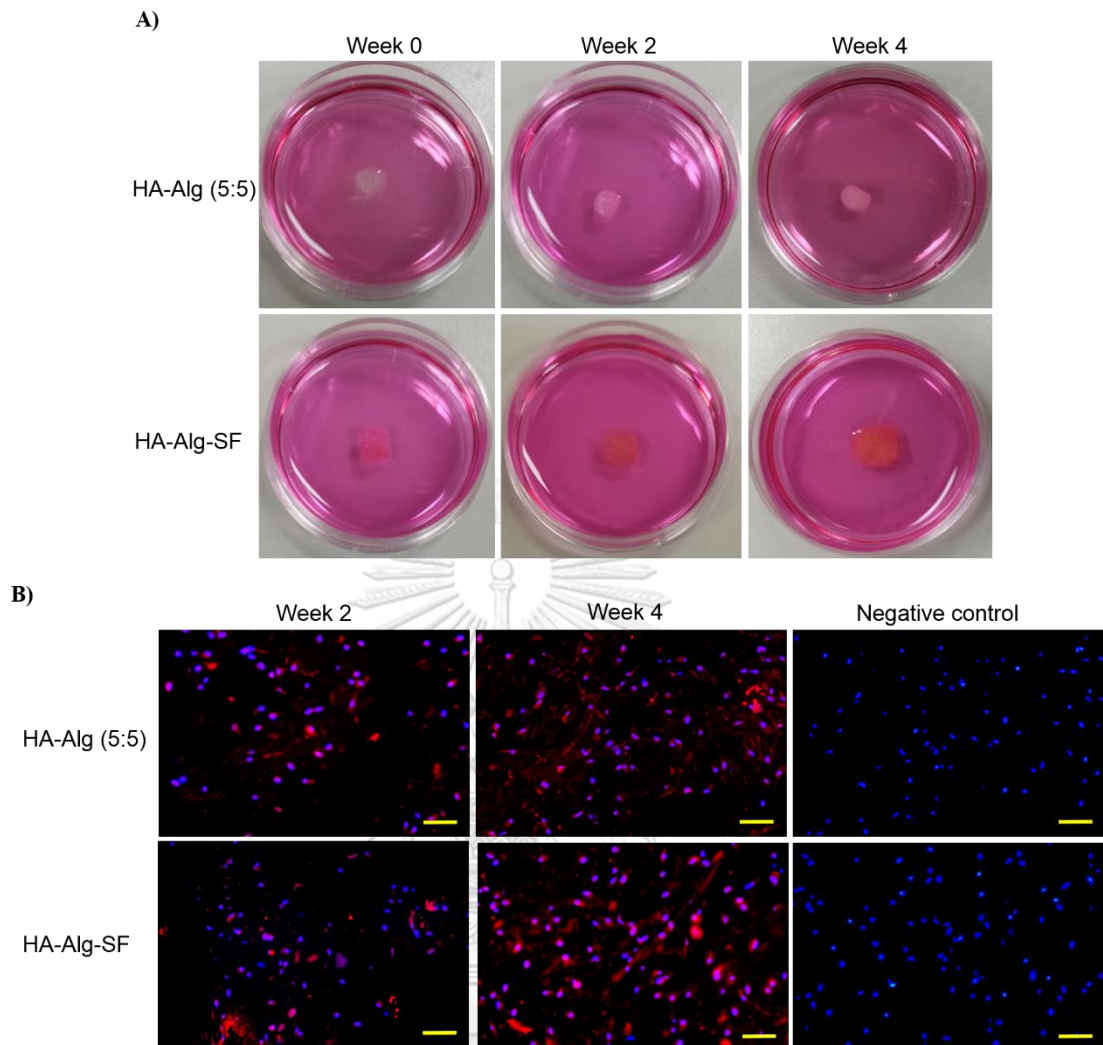


Figure 14. Immunostaining of type II Collagen in HA-Alg (5:5) and HA-Alg-SF hydrogel after 2 weeks and 4 weeks. Negative control was stained without primary antibody (scale: 200 μ m).

CHAPTER 5

CONCLUSION, DISCUSSION, AND RECOMMENDATIONS

5.1 Major findings

The hydrogels were crosslinked by Schiff's base reaction between modified HA-NH₂ and Alg-CHO at different volume ratio (5:5, 6:4, 7:3). The HA-Alg (5:5) was selected as optimal formulation for 3D printing and SF loading due to its rigidity and degradation behavior. It was concluded that the developed hydrogel bioinks facilitated the extrusion-based 3D printing, and played as a supportive matrix for cell encapsulation, proliferation, and chondrogenic differentiation. There was no much difference in printability and biocompatibility between HA-Alg (5:5) and HA-Alg-SF. FTIR spectra show that SF was entangled in the HA-Alg hydrogel system and did not generate new crosslink. This also suggests HA-Alg system is available to load other proteins and growth factors that promote tissue formation after 3D printing.

5.2 Discussion

The four primary 3D printing techniques utilized in tissue engineering are extrusion-based, injek-based, laser-assisted and stereolithography [16, 69, 70]. Among these printing technique, extrusion-based bioprinting is considered as the most common technique in tissue engineering. Extrusion-based bioprinting involves the dispensation of bioink using the extrusion nozzle incorporated with 3D motion. However, choosing a compatible bioink for extrusion-based printing and tissue culture is the primary limitation of 3D bioprinting [25, 71]. Hydrogels are commonly used as bioink thanks to their biocompatibility and viscosity. Viscosity of boink is critical factor that determine the printability and quality of a printed construct, which depends on the chemical components and the concentration of bioink. Viscosity of a hydrogel is determined by its gelation. If the gelation is controllable, the viscosity will be controllable and facilitate 3D printing process [22, 28, 72, 73]. In this research, we aimed to develop a hydrogel bioink comprising natural polymers which are hyaluronic acid, alginate, and silk fibroin. The gelation of bioink was induced by chemical crosslink. This bioink was fabricated in order to facilitate the 3D bioprinting

by extrusion based technique, provide the viability of encapsulating cells, and temperature independence.

Hyaluronic acid, alginate, and silk fibroin have wide applications in field of tissue engineering that mimic the extracellular matrix (ECM) of a variety of hard and soft tissues [34, 40, 74, 75]. These polymers are biocompatible, high biologically active. Alginate and silk fibroin also have good mechanical properties such as long degradation time, high stiffness, which are appropriate for culture of bone and cartilage tissue [8, 76].

Generally, HA, Alg were chemically modified to conjugate amino (-NH₂) and aldehyde (-CHO) functional groups, respectively. The synthesis of HA-NH₂, Alg-CHO have been separately implemented in previous studies, however, the chemical crosslink of HA-NH₂ and Alg-CHO by Schiff's base reaction has not been investigated. In most studies, HA and Alg were crosslinked using Ca²⁺ to perform gelation, which exhibited excellent properties for tissue culture, but its injectability and printability have been unclear [6, 74, 77]. Otherwise, HA-Alg hydrogel produced by Schiff's base reaction showed that it was available for injectability. The injectability of HA-Alg hydrogel by Schiff's base reaction also suggested the printability of HA-Alg hydrogel. SF is a promising biomaterial for 3D printing, but its rheological property is a big challenge due to crosslink conditions [7, 39]. SF was combined with HA, and Alg to fabricate HA-Alg-SF bioink to adjust the rheology of SF in 3D printing and whether improved the physical properties of bioink. In the matrix of HA-Alg-SF, SF was considered as an entangled material, which chemically reacts with neither HA nor Alg. The success in modification of HA and Alg to become HA-NH₂ and Alg-CHO was confirmed by NMR and FTIR spectra results. The HA-Alg and HA-Alg-SF hydrogel crosslink via Schiff's base reaction between amino groups of HA and aldehyde groups of Alg was confirmed through FTIR results.

During the fabrication process, the properties of HA-Alg hydrogels in varied volume ratio was firstly characterized by observe the gelation and injection of each hydrogels through 18G syringe nozzle. Three volume ratio of HA-NH₂ and Alg-CHO (5:5, 6:4, 7:3) can perform gelation. The HA-Alg (5:5) hydrogels was more rigid than 6:4 and 7:3 hydrogels, while 7:3 hydrogels were soft and aqueous. For 3D printing, obviously,

the 5:5 hydrogels was highly preferable for maintaining the printed constructs after printing.

Next, the swelling and degradation of HA-Alg hydrogel (5:5, 6:4, 5:5) were determined. The data indicated that the HA-Alg hydrogel with the volume ratio 5:5 was more stable than the other ratios during 5 weeks, and much slowly degraded. Since we aimed to investigate a hydrogel bioink for 3D printing and the HA-Alg (5:5) has appeared to achieve the best gel structure and degradation behavior for cell culture, we selected the HA-Alg (5:5) as optimal formulation for 3D printing and combined with SF. The HA-Alg-SF hydrogels were fabricated with 2% wt SF in its formulation. From our previous study, SF was combined with Alg to produce Alg-SF hydrogel in varied SF concentration. It was noted that 2% wt SF was optimal for cell viability and proliferation [42]. The gelation, swelling, and degradation of HA-Alg-SF hydrogels were also examined together with HA-Alg. Further examinations on the HA-Alg (5:5) and HA-Alg-SF were subsequently studied in 3D printing and their biocompatibility.

The HA-Alg (5:5) and HA-Alg-SF hydrogels were applied as bioink for screw extrusion based 3D printing, using our custom-made 3D printer (Enterprise 2.0), which indicated that the viscosity of HA-Alg (5:5) and HA-Alg-SF hydrogels favored printing process and allowed the 3D construct formation after printing. The HA-Alg (5:5) and HA-Alg-SF hydrogels were mixed with hMSCs before printing, the results from live/dead staining showed that a large number of cell alive after printing. We also conducted the experiments on the HA-Alg (5:5) and HA-Alg-SF hydrogels' physical properties and biocompatibility with human mesenchymal stem cells (hMSCs).

Mechanical properties of HA-Alg (5:5) and HA-Alg-SF hydrogels including compressive strength and rheology were investigated. Both HA-Alg (5:5) and HA-Alg-SF hydrogels exhibited elastic behavior ($G' > G''$). The gelation point could not recorded due to the quick reaction between HA-NH₂ and Alg-CHO, this revealed that these hydrogels could quickly prepare for 3D printing and it will allow homogenous cell distribution when mixing cells with bioink. HA-Alg (5:5) and HA-Alg-SF hydrogels were available for 3D extrusion through a small syringe needle.

Biocompatibility of HA-ALg (5:5) and HA-Alg-SF hydrogels were tested by live/dead, PrestoBlue™, Quant-iT™ Picogreen™ dsDNA, and Ki-67 immunostaining to assess the toxicity and cell proliferation.

According to ISO standard 10993-5:2009, live/dead assay was carried out to observe the cell distribution in the hydrogels using Calcein-AM/ EthD-1 staining. Both HA-ALg (5:5) and HA-Alg-SF hydrogels were highly biocompatible. Since large number of cell encapsulated in the hydrogels at the beginning (10^6 cells/mL), there were large population of alive cells and insignificant number of dead cells observed during 7 days, and the increase in cell number due to proliferation was not obvious in 3D structure. Therefore, cell proliferation in HA-ALg (5:5) and HA-Alg-SF cultured in 1, 3, and 7 days, was assessed by Quant-iT™ Picogreen™ dsDNA and PrestoBlue™ assay. The results from these two experiments confirmed that there was cell increase in the hydrogels during culture period, whereas HA-ALg hydrogel had a greater cell viability than HA-Alg-SF. In Quant-iT™ Picogreen™ dsDNA and PrestoBlue™ assay, to ensure the recorded data were relevant to 3D cell culture, the control sample was another 3D hydrogel that was highly biocompatible from previous studies. Here, we selected fibrin hydrogel. Fibrin hydrogel was fabricated from gelatin, fibrinogen, hyaluronic acid, glycerol and crosslinked by thrombin. This hydrogels showed excellent biological activities for many cell types and tissues[55]. In our experiments, Fibrin hydrogel was gold standard to act as control sample.

The data collected showed the physical and biocompatible properties of HA-ALg and HA-Alg-SF bioinks. To prove that this bioink can go further for tissue culture, hMSCs were induced chondrogenic differentiation in 3D HA-ALg (5:5) and HA-ALg-SF hydrogels. The success in Collagen-II staining after 4 weeks confirmed that HA-ALg and HA-ALg-SF hydrogels could be active bioinks for cartilage 3D printing. Not only for cartilage, HA, Alg, and SF could be used for many types of tissue. HA-ALg could be considered as a based bioink for 3D printing. The addition of SF in the HA-ALg network suggests the loading of other proteins, growth factor or a third material in the HA-ALg to promote a specific 3D printed tissue.

For scaling up the experiment, the degree of chemical modification and crosslinked hydrogels will be measured and controlled by Mass Spectroscopy, to ensure the repeatability and reproducibility of the bioinks.

5.3 Limitation of the study

This study currently stands by in vitro characterization.

Animal tests with the bioinks should be further conducted to understand more about their functions and overall effects in live subjects.



REFERENCES

1. Howard, D., et al., *Tissue engineering: strategies, stem cells and scaffolds*. Journal of anatomy, 2008. **213**(1): p. 66-72.
2. Gungor-Ozkerim, P.S., et al., *Bioinks for 3D bioprinting: an overview*. Biomaterials science, 2018. **6**(5): p. 915-946.
3. Gelinsky, M., 6 - *Biopolymer hydrogel bioinks*, in *3D Bioprinting for Reconstructive Surgery*, D.J. Thomas, Z.M. Jessop, and I.S. Whitaker, Editors. 2018, Woodhead Publishing. p. 125-136.
4. Bulpitt, P. and D. Aeschlimann, *New strategy for chemical modification of hyaluronic acid: preparation of functionalized derivatives and their use in the formation of novel biocompatible hydrogels*. J Biomed Mater Res, 1999. **47**(2): p. 152-69.
5. Jejurikar, A., et al., *Degradable alginate hydrogels crosslinked by the macromolecular crosslinker alginate dialdehyde*. J. Mater. Chem., 2012. **22**: p. 9751-9758.
6. Antich, C., et al., *Bio-inspired hydrogel composed of hyaluronic acid and alginate as a potential bioink for 3D bioprinting of articular cartilage engineering constructs*. Acta Biomaterialia, 2020. **106**: p. 114-123.
7. Wang, Q., et al., *3D Printing of Silk Fibroin for Biomedical Applications*. Materials (Basel, Switzerland), 2019. **12**(3): p. 504.
8. Murphy, A.R. and D.L. Kaplan, *Biomedical applications of chemically-modified silk fibroin*. Journal of materials chemistry, 2009. **19**(36): p. 6443-6450.
9. Frantz, C., K.M. Stewart, and V.M. Weaver, *The extracellular matrix at a glance*. Journal of cell science, 2010. **123**(Pt 24): p. 4195-4200.
10. Reiser, K.M., *Extracellular Matrix*, in *Encyclopedia of Gerontology (Second Edition)*, J.E. Birren, Editor. 2007, Elsevier: New York. p. 555-564.
11. Moon, B.M., et al., *Novel fabrication method of the peritoneal dialysis filter using silk fibroin with urease fixation system*. Journal of Biomedical Materials Research Part B: Applied Biomaterials, 2017. **105**(7): p. 2136-2144.
12. Zhao, P., et al., *Fabrication of scaffolds in tissue engineering: A review*. Frontiers of Mechanical Engineering, 2018. **13**(1): p. 107-119.
13. Pezeshki-Modaress, M., et al., *Cell-loaded gelatin/chitosan scaffolds fabricated by salt-leaching/lyophilization for skin tissue engineering: in vitro and in vivo study*. J Biomed Mater Res A, 2014. **102**(11): p. 3908-17.
14. Chia, H.N. and B.M. Wu, *Recent advances in 3D printing of biomaterials*. Journal of Biological Engineering, 2015. **9**(1): p. 4.
15. Gopinathan, J. and I. Noh, *Recent trends in bioinks for 3D printing*. Biomaterials research, 2018. **22**: p. 11-11.
16. Yan, Q., et al., *A Review of 3D Printing Technology for Medical Applications*. Engineering, 2018. **4**(5): p. 729-742.
17. El Aita, I., J. Breitzkreutz, and J. Quodbach, *On-demand manufacturing of immediate release levetiracetam tablets using pressure-assisted microsyringe printing*. European Journal of Pharmaceutics and Biopharmaceutics, 2018. **134**.
18. Azad, M.A., et al., *Polymers for Extrusion-Based 3D Printing of Pharmaceuticals: A Holistic Materials-Process Perspective*. Pharmaceutics, 2020. **12**(2).

19. Placone, J.K. and A.J. Engler, *Recent Advances in Extrusion-Based 3D Printing for Biomedical Applications*. *Advanced healthcare materials*, 2018. **7**(8): p. e1701161-e1701161.
20. Cuiffo, M., et al., *Impact of the Fused Deposition (FDM) Printing Process on Polylactic Acid (PLA) Chemistry and Structure*. *Applied Sciences*, 2017. **7**: p. 579.
21. Panwar, A. and L.P. Tan, *Current Status of Bioinks for Micro-Extrusion-Based 3D Bioprinting*. *Molecules (Basel, Switzerland)*, 2016. **21**(6): p. 685.
22. Wang, X., et al., *Gelatin-Based Hydrogels for Organ 3D Bioprinting*. *Polymers*, 2017. **9**: p. 401.
23. Gao, T., et al., *Optimization of gelatin-alginate composite bioink printability using rheological parameters: a systematic approach*. *Biofabrication*, 2018. **10**(3): p. 034106-034106.
24. Blaeser, A., et al., *Controlling Shear Stress in 3D Bioprinting is a Key Factor to Balance Printing Resolution and Stem Cell Integrity*. *Advanced healthcare materials*, 2015. **5**.
25. Willson, K., et al., *Extrusion-Based Bioprinting: Current Standards and Relevancy for Human-Sized Tissue Fabrication*, in *3D Bioprinting: Principles and Protocols*, J.M. Crook, Editor. 2020, Springer US: New York, NY. p. 65-92.
26. Montero, F.E., et al., *Development of a Smart Bioink for Bioprinting Applications*. *Frontiers in Mechanical Engineering*, 2019. **5**(56).
27. Jeon, O., et al., *Cryopreserved cell-laden alginate microgel bioink for 3D bioprinting of living tissues*. 2019.
28. Ramiah, P., et al., *Hydrogel-Based Bioinks for 3D Bioprinting in Tissue Regeneration*. *Frontiers in Materials*, 2020. **7**(76).
29. Xu, C., et al., *Highly Elastic Biodegradable Single-Network Hydrogel for Cell Printing*. *ACS applied materials & interfaces*, 2018. **10**(12): p. 9969-9979.
30. Zhu, J. and R.E. Marchant, *Design properties of hydrogel tissue-engineering scaffolds*. *Expert review of medical devices*, 2011. **8**(5): p. 607-626.
31. Grover, C.N., et al., *Crosslinking and composition influence the surface properties, mechanical stiffness and cell reactivity of collagen-based films*. *Acta biomaterialia*, 2012. **8**(8): p. 3080-3090.
32. Paidikondala, M., et al., *Impact of Hydrogel Cross-Linking Chemistry on the in Vitro and in Vivo Bioactivity of Recombinant Human Bone Morphogenetic Protein-2*. *ACS Applied Bio Materials*, 2019. **2**(5): p. 2006-2012.
33. Porter, D. and F. Vollrath, *Silk as a Biomimetic Ideal for Structural Polymers*. *Advanced Materials*, 2009. **21**(4): p. 487-492.
34. Müller, M., et al., *Alginate Sulfate–Nanocellulose Bioinks for Cartilage Bioprinting Applications*. *Annals of Biomedical Engineering*, 2016. **45**.
35. Galarraga, J.H., M.Y. Kwon, and J.A. Burdick, *3D bioprinting via an in situ crosslinking technique towards engineering cartilage tissue*. *Scientific Reports*, 2019. **9**(1): p. 19987.
36. Brenckle, M.A., et al., *Protein-protein nanoimprinting of silk fibroin films*. *Advanced materials (Deerfield Beach, Fla.)*, 2013. **25**(17): p. 2409-2414.
37. DeSimone, E., et al., *Recombinant spider silk-based bioinks*. *Biofabrication*, 2017. **9**(4): p. 044104.
38. Jose, R.R., et al., *Polyol-Silk Bioink Formulations as Two-Part Room-*

- Temperature Curable Materials for 3D Printing*. ACS Biomaterials Science & Engineering, 2015. **1**(9): p. 780-788.
39. Chawla, S., et al., *Silk-Based Bioinks for 3D Bioprinting*. Advanced Healthcare Materials, 2018. **7**: p. 1701204.
 40. Singh, Y.P., *3D Bioprinting Using Cross-Linker-Free Silk-Gelatin Bioink for Cartilage Tissue Engineering*. 2019. **11**(37): p. 33684-33696.
 41. Chameettachal, S., S. Midha, and S. Ghosh, *Regulation of Chondrogenesis and Hypertrophy in Silk Fibroin-Gelatin-Based 3D Bioprinted Constructs*. ACS Biomaterials Science & Engineering, 2016. **2**(9): p. 1450-1463.
 42. Nguyễn, T.T., J. Ratanavaraporn, and S. Yodmuang. *Alginate-silk fibroin Bioink : A printable hydrogel for tissue engineering*. in *2019 12th Biomedical Engineering International Conference (BMEiCON)*. 2019.
 43. Marques, C., et al., *Collagen-based bioinks for hard tissue engineering applications: a comprehensive review*. Journal of Materials Science: Materials in Medicine, 2019. **30**.
 44. Petta, D., et al., *Hyaluronic acid as a bioink for extrusion-based 3D printing*. Biofabrication, 2020. **12**(3): p. 032001.
 45. Camci-Unal, G., et al., *Synthesis and characterization of hybrid hyaluronic acid-gelatin hydrogels*. Biomacromolecules, 2013. **14**(4): p. 1085-1092.
 46. O'Connell, C., et al., *Evaluation of sterilisation methods for bio-ink components: gelatin, gelatin methacryloyl, hyaluronic acid and hyaluronic acid methacryloyl*. Biofabrication, 2019. **11**.
 47. Yin, J., et al., *3D bioprinting of low concentration cell-laden gelatin methacrylate (GelMA) bioinks with two-step crosslinking strategy*. ACS Applied Materials & Interfaces, 2018. **10**.
 48. Petta, D., et al., *3D bioprinting of a hyaluronan bioink through enzymatic- and visible light- crosslinking*. Biofabrication, 2018. **10**.
 49. Petta, D., et al., *3D printing of a tyramine hyaluronan derivative with double gelation mechanism for independent tuning of shear thinning and post-printing curing*. ACS Biomaterials Science & Engineering, 2018. **4**.
 50. Lee, K.Y. and D.J. Mooney, *Alginate: properties and biomedical applications*. Progress in polymer science, 2012. **37**(1): p. 106-126.
 51. Gao, C., et al., *Preparation of Sodium Alginate Hydrogel and Its Application in Drug Release*. Progress in Chemistry, 2013. **25**: p. 1012-1022.
 52. Wang, J., et al., *3D printed agar/ calcium alginate hydrogels with high shape fidelity and tailorable mechanical properties*. Polymer, 2021. **214**: p. 123238.
 53. Tan, H., et al., *Controlled gelation and degradation rates of injectable hyaluronic acid-based hydrogels through a double crosslinking strategy*. Journal of tissue engineering and regenerative medicine, 2011. **5**(10): p. 790-797.
 54. Lerdchai, K., et al., *Thai Silk Fibroin/Gelatin Sponges for the Dual Controlled Release of Curcumin and Docosahexaenoic Acid for Anticancer Treatment*. J Pharm Sci, 2016. **105**(1): p. 221-30.
 55. Kang, H.-W., et al., *A 3D bioprinting system to produce human-scale tissue constructs with structural integrity*. Nature Biotechnology, 2016. **34**: p. 312.
 56. Youm, I., et al., *Uptake and Cytotoxicity of Docetaxel-Loaded Hyaluronic Acid-Grafted Oily Core Nanocapsules in MDA-MB 231 Cancer Cells*. Pharmaceutical research, 2014. **31**.

57. Snyder, T., et al., *Erratum to: A fibrin/hyaluronic acid hydrogel for the delivery of mesenchymal stem cells and potential for articular cartilage repair*. Journal of biological engineering, 2014. **8**: p. 10.
58. Wang, L., et al., *Magnetic Fullerene-DNA/Hyaluronic Acid Nanovehicles with Magnetism/Reduction Dual-Responsive Triggered Release*. 2017. **18 3**: p. 1029-1038.
59. MacDonald, L. and B. Berger, *A Polysaccharide Lyase from Stenotrophomonas maltophilia with a Unique, pH-regulated Substrate Specificity*. The Journal of biological chemistry, 2013. **289**.
60. Wang, L., et al., *Preparation and catalytic performance of alginate-based Schiff Base*. Carbohydrate Polymers, 2019. **208**: p. 42-49.
61. Córdova, B., et al., *Chemical modification of alginate with thiosemicarbazide for the removal of Pb(II) and Cd(II) from aqueous solutions*. International Journal of Biological Macromolecules, 2018. **120**.
62. Rinawati, L., et al., *Increasing the effectiveness of pesticides based urea nanofertilizer encapsulated nanosilica with addition of rice husk TiO₂ additive substances*. Journal of Chemical and Pharmaceutical Research, 2015. **2015**: p. 85-89.
63. Qiao, L., et al., *Self-healing alginate hydrogel based on dynamic acylhydrazone and multiple hydrogen bonds*. Journal of Materials Science, 2019. **54**.
64. Hassan, M.A., et al., *Preparation, physicochemical characterization and antimicrobial activities of novel two phenolic chitosan Schiff base derivatives*. Scientific Reports, 2018. **8**: p. 11416.
65. Hölzl, K., et al., *Bioink properties before, during and after 3D bioprinting*. Biofabrication, 2016. **8**(3): p. 032002.
66. Kyle, S., et al., *'Printability' of Candidate Biomaterials for Extrusion Based 3D Printing: State-of-the-Art*. Adv Healthc Mater, 2017. **6**(16).
67. Lall, N., et al., *Viability Reagent, PrestoBlue, in Comparison with Other Available Reagents, Utilized in Cytotoxicity and Antimicrobial Assays*. International journal of microbiology, 2013. **2013**: p. 420601-420601.
68. Sun, X. and P.D. Kaufman, *Ki-67: more than a proliferation marker*. Chromosoma, 2018. **127**(2): p. 175-186.
69. Bishop, E.S., et al., *3-D bioprinting technologies in tissue engineering and regenerative medicine: Current and future trends*. Genes & diseases, 2017. **4**(4): p. 185-195.
70. Ozbolat, I.T., W. Peng, and V. Ozbolat, *Application areas of 3D bioprinting*. Drug Discov Today, 2016. **21**(8): p. 1257-71.
71. Leucht, A., et al., *Advanced gelatin-based vascularization bioinks for extrusion-based bioprinting of vascularized bone equivalents*. Scientific reports, 2020. **10**(1): p. 5330-5330.
72. Blaeser, A., D.F. Duarte Campos, and H. Fischer, *3D bioprinting of cell-laden hydrogels for advanced tissue engineering*. Current Opinion in Biomedical Engineering, 2017. **2**: p. 58-66.
73. Stanton, M., J. Samitier, and S. Sánchez, *Bioprinting of 3D Hydrogels*. Lab on a chip, 2015. **15**.
74. Rubert, M., et al., *Evaluation of Alginate and Hyaluronic Acid for Their Use in Bone Tissue Engineering*. Biointerphases, 2012. **7**: p. 44-55.

75. Gilarska, A., et al., *Collagen/chitosan/hyaluronic acid – based injectable hydrogels for tissue engineering applications – design, physicochemical and biological characterization*. *Colloids and Surfaces B: Biointerfaces*, 2018. **170**.
76. Ziv, K., et al., *A tunable silk–alginate hydrogel scaffold for stem cell culture and transplantation*. *Biomaterials*, 2014. **35**.
77. Lee, S.J., et al., *Three-Dimensional Printable Hydrogel Using a Hyaluronic Acid/Sodium Alginate Bio-Ink*. 2021. **13**(5): p. 794.



VITA

NAME	Truc Thanh Nguyen
DATE OF BIRTH	31 January 1996
PLACE OF BIRTH	Vietnam
INSTITUTIONS ATTENDED	International University-Vietnam National University, HCMC.
HOME ADDRESS	Ho Chi Minh City, Vietnam



จุฬาลงกรณ์มหาวิทยาลัย
CHULALONGKORN UNIVERSITY